UNITED NATIONS UNIVERSITY

GEOTHERMAL TRAINING PROGRAMME
Orkustofnun, Grensasvegur 9,
IS-108 Reykjavik, Iceland

Reports 2013
Number 2

BOREHOLE GEOLOGY AND HYDROTHERMAL MINERALISATION OF WELL OW-37A, OLKARIA EAST GEOTHERMAL FIELD, KENYA

Victor Otieno and Rose Kubai
Kenya Electricity Generating Company Ltd. – KenGen
P.O. Box 785-20117
Naivasha
KENYA
votieno@kengen.co.ke; rkubai@kengen.co.ke

ABSTRACT

Well OW-37A is a production well located in the Olkaria East Field, located within the Olkaria geothermal system. It is a directional well drilled towards northwest to a total depth of 2848 m according to cellar table (CT). The well was drilled as a production well to supply steam to Olkaria 1 power plant's additional units 4 and 5. Production casing was set at 746 m CT. Detailed binocular and petrographic analysis reveals five distinct lithologic units, namely pyroclastics, rhyolite, tuff, basalt and trachyte. The latter forms the bulk of the stratigraphy and is predominant below 752 m down to 2848 m. Drilling of the well lasted for 56 days, beginning 31st March 2009 and ending 25th May. Hydrothermal alteration mineral assemblages occur systematically with increasing temperature and depth. Five hydrothermal alteration zones were identified: an unaltered zone, a zeolite-chlorite-illite zone, a chlorite-illite zone, an epidote-chlorite-illite zone and an actinolite-epidote zone. Six small and seven medium feed zones were noted, associated mainly with circulation losses. The three major aquifers are associated with circulation losses, fracturing and high-grade alteration and can be deduced from large deflections in the temperature profile as shown by large peaks. In summary, the permeability of the well is generally good. A fluid inclusion analysis, using 52 inclusions from quartz and calcite collected at 668-670 m depth, established two temperature populations in the well at 205-220°C and 230-245°C. A comparison of homogenization temperature (T_h) and the measured formation temperature indicates the system has been in a dynamic state where temperatures have changed through time. The 230-245°C regime of inclusions is in equilibrium with existing reservoir temperatures. In contrast, a comparison of alteration temperature and measured formation temperature indicates the system around the well to be cooling in the uppermost 600 m and heating up below 600 m depth.

1. INTRODUCTION

1.1 General information

The Greater Olkaria geothermal area (GOGA) is situated south of Lake Naivasha, approximately 120 km from Nairobi on the floor of the southern segment of the Kenya rift (Figure 1). The Kenya rift is an

integral part of the East African Rift System, which extends for over 3000 km from the Afar triple junction at the Gulf of Eden in the north to Beira, Mozambique in the south. It is the segment of the eastern arm of the rift extending from Lake Turkana to the North to Lake Natron, N-Tanzania to the south. The rift is a classic example of a continental divergent zone where spreading occurs resulting in the thinning of the crust, hence the eruption of lavas and associated volcanic activities.

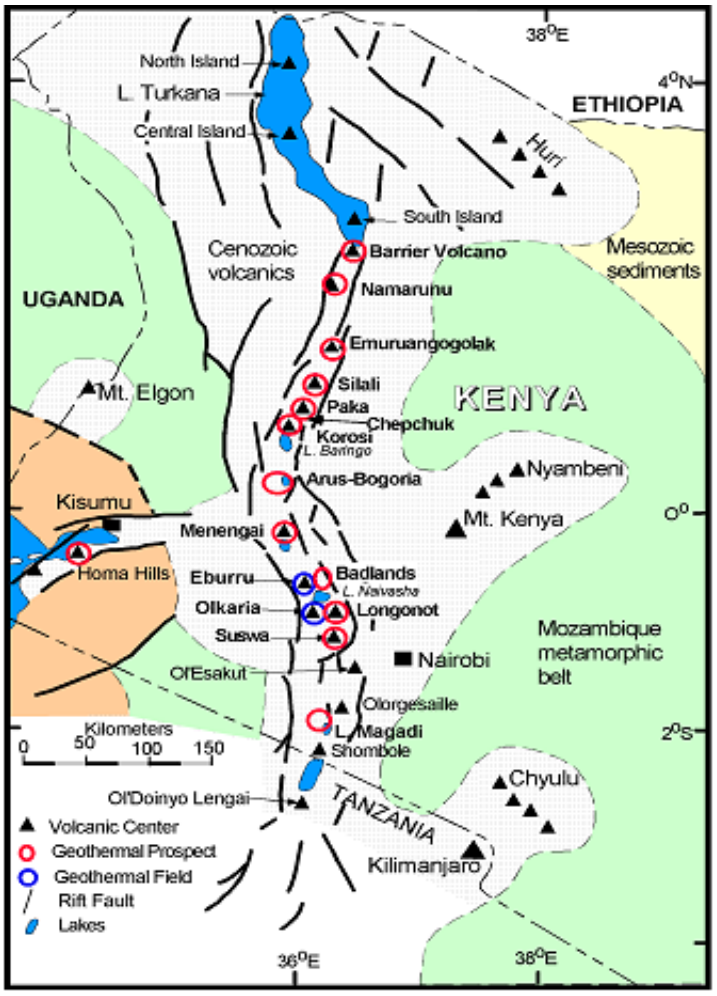

FIGURE 1: Map showing the location of the Greater Olkaria geothermal area and other volcanic and geothermal centres (Ofwona, 2010)

The Olkaria geothermal system lies within the Greater Olkaria volcanic complex (GOVC). The Greater Olkaria geothermal area covers approximately 140 km^2 and is subdivided into seven fields for purposes of geothermal development (Mwangi, 2000). These include Olkaria East, Olkaria Northeast, Olkaria Central, Olkaria Northwest, Olkaria Southwest, Olkaria Southeast and Olkaria Domes (Figure 2). All these production fields are named with reference to Olkaria Hill.

Exploration of the Olkaria Geothermal field commenced in 1956 with the drilling of two wells (X-1 and X-2, but they proved unproductive. In 1971 and 1972, a surface exploration programme was undertaken, jointly funded by the Kenya Government and the United Nations (Mwangi, 2000). This resulted in the drilling of a number of exploration wells during the period 1972-1976.

The Olkaria East field (Olkaria I), which is the field of focus in this study, has been producing power since 1981 when the first of the three 15 MWe units was commissioned; two others (units II and III) were commissioned in 1982 and 1985, respectively. The current generating capacity of the field is 45 MWe. Currently, additional units (Olkaria I units IV and V) each with a generational capacity of 70 MWe are under construction and are due for commissioning in 2014. Olkaria Northeast field (Olkaria II) is generating 105 MWe, and Olkaria Northwest field (Olkaria III) which is being developed by an Independent Power Producer (IPP) is currently producing 48 MWe.

In the Olkaria Domes field, at the Olkaria IV power plant, two units (units I and II), is under construction, each unit with a production capacity of 70 MWe. They are due for commissioning in 2014. The rest of the fields are at various exploration stages.

1.2 Objective of the study

The main objective of this project is to study the borehole geology of well OW-37A (Figure 3) in detail through analysis of drill cuttings in order to:

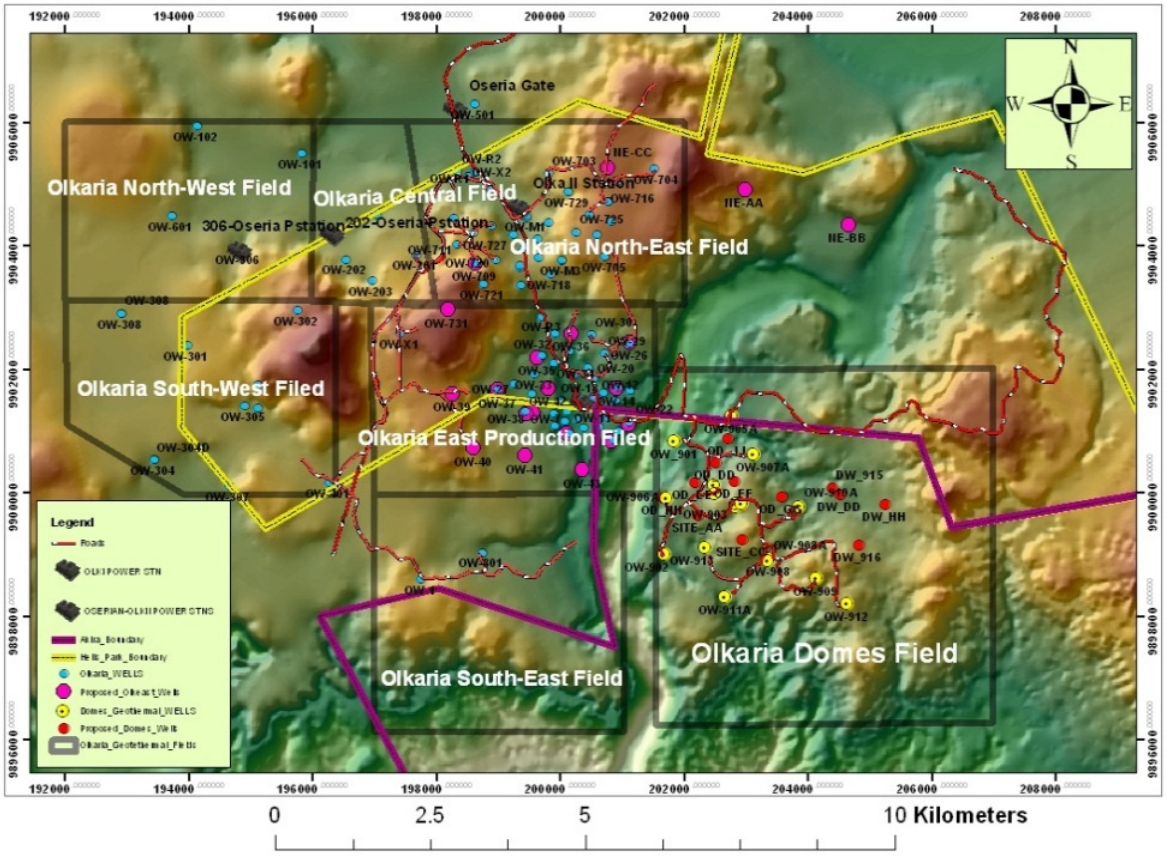

FIGURE 2: Map of the Greater Olkaria geothermal area showing Olkaria geothermal fields

- Identify the subsurface lithologic units;
- Locate the aquifers or feed zones;
- Determine the alteration and hydrothermal mineral assemblages; and
- Understand the reservoir conditions of the area.

This project report was prepared and submitted as a requirement for the fulfilment and attainment of the three month *Course on Geothermal Technology* and the six month *Advanced Training in Borehole Geology* organised by the United Nations University Geothermal Training Programme (UNU-GTP) in the period 16th April, 2012 to 1st February, 2013.

2. GEOLOGY

2.1 Regional geology

As discussed earlier, the Olkaria volcanic system is located south of Lake Naivasha on the southern segment of the Kenya Rift. The Kenyan Rift is a divergent plate boundary, where the Somali and Nubian plates are drifting apart at an average rate of about 2 cm per year, thus creating a thinner crust (KenGen, 1998). The evolution of the East African Rift System is structurally controlled, with the rift faults exploiting the weak collisional zone at the contact between the Archean Tanzanian craton and the Proterozoic orogenic belts (Smith and Mosley, 1993). It has been determined that rifting activities in the Kenyan rift began during the late Oligocene to early Miocene to the north around Lake Turkana, in an area known as the Turkana Rift and propagated southwards to the central segment (Omenda, 1998).

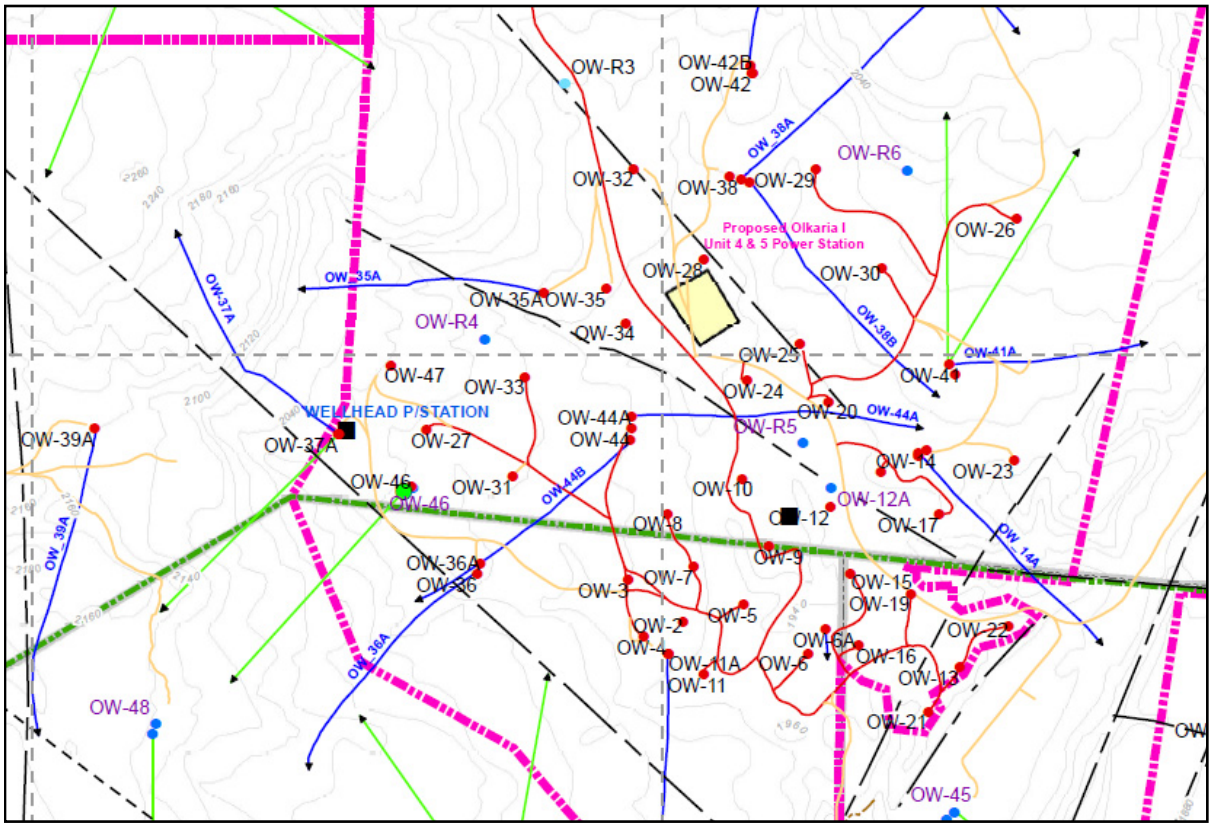

FIGURE 3: Sketch map showing the location of well OW-37A in Olkaria

Rift tectonism has resulted in intense volcanism in the rift and numerous volcanic centres in the Central Kenya Rift, associated with Quaternary silicic volcanism (Muchemi, 1999; Omenda, 1998). Extensive eruptions of basaltic and phonolitic rocks occurred during the Miocene, preceded by the uplift of the Kenya dome. Rift faulting began during late Miocene resulting in eruptions of large volumes of Pliocene ignimbritic tuffs within the developing graben structure in the central segment of the rift, forming the Mau and Kinangop tuffs. Subsequent faulting episodes succeeding the ignimbrite volcanism gave rise to major rift-bounding faults. In the developing graben, the formation of plateau trachyte rocks, namely trachytes, basalts, basaltic trachy-andesites, and trachy-andesites, occurred through fissure eruptions during the early Pleistocene (Lagat, 2005). The plateau rocks filling the developing graben were subsequently block-faulted to create high-angle normal faults within the rift floor. The resulting fractures, a common feature of the rift floor, apparently served as conduits for the Quaternary volcanics of mafic to felsic composition. The youngest volcanic suites of the rift-fill include Pleistocene-Holocene rhyolites, trachytes, basalts, phonolites, and pyroclastics (Thompson and Dodson, 1963; Naylor, 1972; Baker and Wohlenberg, 1971, Baker et al., 1972; Odongo, 1986; Clarke et al., 1990).

2.2 Geology of the Greater Olkaria volcanic complex (GOVC)

The regional geology and stratigraphy of the Greater Olkaria volcanic complex has been discussed in detail by Clarke et al. (1990). The Greater Olkaria volcanic complex is a multi-centred volcanic field characterized by numerous volcanic centres of Quaternary age (Macdonald et al., 1987). The volcanic centres occur as steep-sided domes formed by lavas and/or pyroclastics, or as thick lava flows of restricted lateral extent. Lagat (2004) noted that the Olkaria volcanic complex is the only area within the Great Kenyan rift with the occurrence of comenditic lava on the surface. Other Quaternary volcanic centres adjacent to the Greater Olkaria volcanic complex include: Eburru to the north, Longonot to the east, and Suswa to the south (Figure 1). Although these neighbouring volcanic suites

have discernible caldera associations, the Olkaria volcanic complex does not have an explicit caldera. However, surface mapping by Naylor (1972) identified the Olkaria volcanic complex as the remnant of an old caldera complex, marked by the presence of a ring of volcanic domes in the east, south and southwest of this complex.

Seismic wave attenuation studies for the entire Olkaria area have also indicated an anomaly in the area coinciding with the proposed caldera (Simiyu, 1998; Simiyu et al., 1998). On the other hand, additional studies in Olkaria, such as resistivity studies (Onacha, 1993) and subsurface geology, and e.g. the absence of ignimbrites in Olkaria (Omenda, 1998), have failed to positively establish the presence of a buried caldera.

The surface geology of the Olkaria volcanic complex is dominated by comendites and pyroclastic fall deposits (pumice fall and ash deposits) (Figure 4). The subsurface geology of the Olkaria geothermal field can be divided into six broad lithostratigraphic groups based on age, tectono-stratigraphy, and lithology, as revealed by data from more than eighty deep wells in the geothermal area (Omenda, 2000). The formations are the Proterozoic "basement" formations, Mau tuffs, plateau trachytes, Olkaria basalts, and Upper Olkaria volcanics (Figure 5). A brief discussion of the defined groups based on chrono-graphic order from the oldest to youngest is given hereunder.

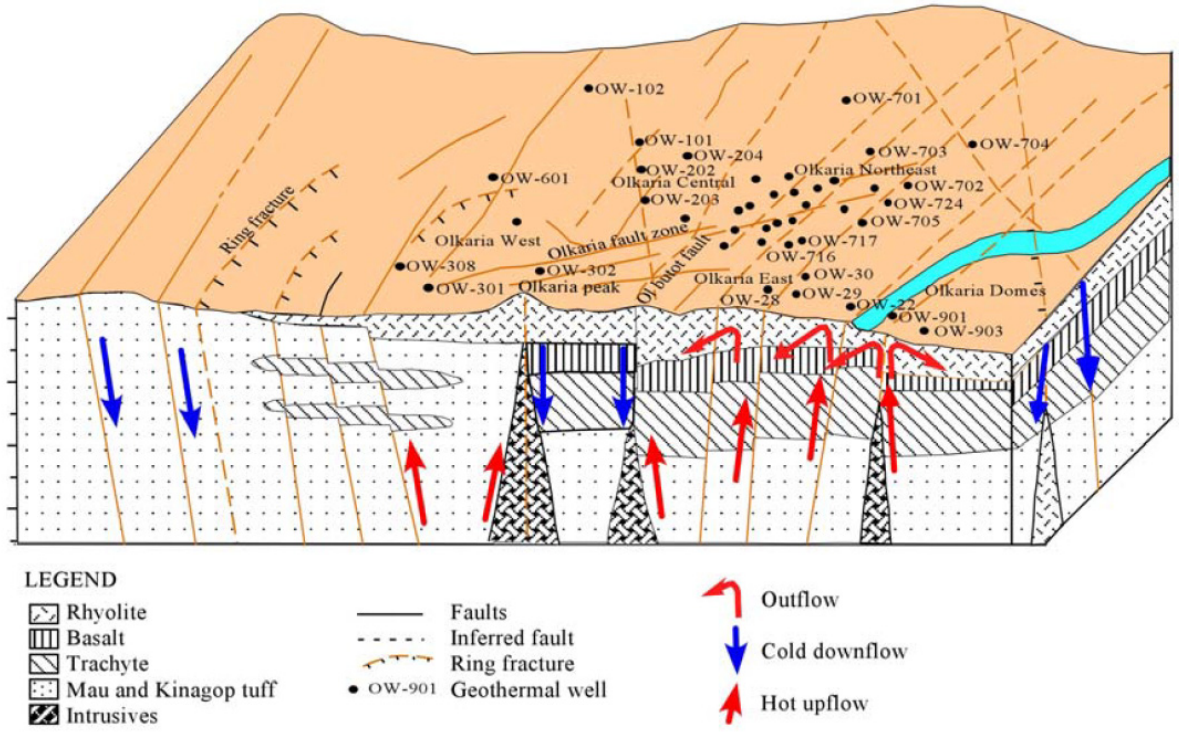

FIGURE 4: Updated conceptual model showing general geology of the Greater Olkaria area

The Mau tuffs are considered to be the oldest rocks encountered in the Olkaria area and are common on the surface in the area west of Olkaria Hill, but are absent in the east field due to an east high-dipping high-angle normal fault traversing Olkaria Hill (Figure 4). The rocks that comprise the Mau Tuffs are trachytes, basalts and ignimbrites and are of unknown thickness (Omenda, 1994, 1998). The rocks vary in texture from consolidated to ignimbritic and are the main geothermal reservoir rocks in the Olkaria West field as based on the drill cuttings from the geothermal boreholes in the area.

The plateau trachytes are of Pleistocene age and are predominantly composed of trachytic lavas with minor basalts, tuffs and rhyolites. This formation hosts the geothermal reservoirs for the Olkaria East and Northeast fields. The thickness of the formation is estimated to be more than 1.5 km as indicated

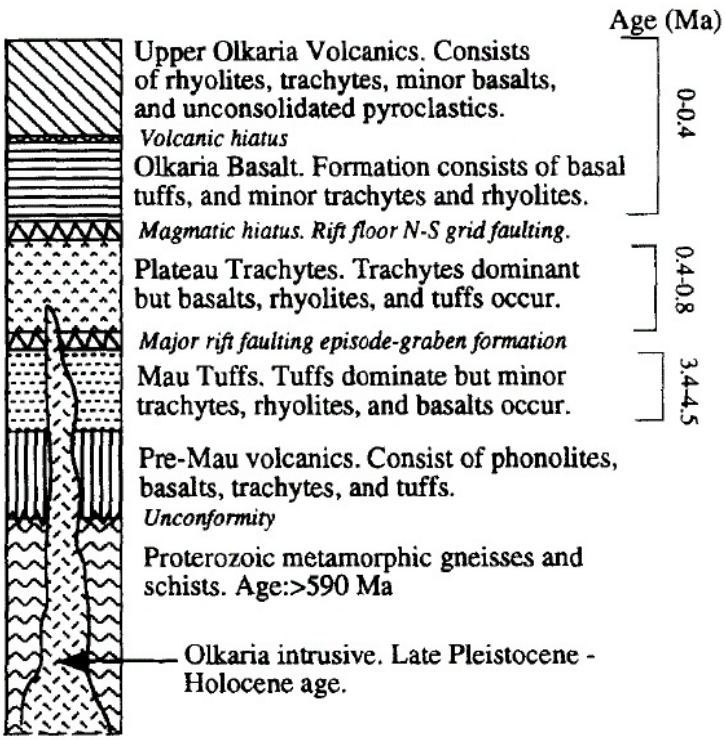

FIGURE 5: Lithostratigraphic column of the Olkaria volcanic complex (Omenda, 1998)

by the boreholes drilled in the East field, which have not encountered the underlying Mau Tuffs at depths of up to 2600 m (Odongo, 1986, Omenda, 1994).

Olkaria basalt consists of basaltic flows, minor pyroclastic deposits and trachytes. It is believed to form the cap-rock for the Olkaria geothermal system (Haukwa, 1984; Ambusso and Ouma, 1991). The formation varies in thickness from 100 m to 500 m underlying the Upper Olkaria volcanics.

The Olkaria basalt formation underlies the Upper Olkaria volcanics and is composed of numerous thin basaltic flows separated by thin layers of tuffs, minor trachytes, and occasional rhyolites. The formation has been penetrated by nearly all wells in the East and Northeast Olkaria fields at nearly constant elevation, and varies in thickness between 100 and 400 m. However, this formation is conspicuously absent in the West field. According to hydrothermal studies (Browne, 1984a and b; Leach and Muchemi, 1987; Muchemi, 1992; Omenda, 1998) and reservoir modelling (Haukwa, 1984; Ambusso and Ouma, 1991), the Olkaria basaltic formation is considered to act as cap-rock for the Olkaria geothermal system. This fact has been supported by the sharp temperature increases occurring below the formation.

The Upper Olkaria formation consists of comendite lavas and their pyroclastic equivalents, ashes from Suswa and Longonot volcanoes and minor trachytes and basalts (Thompson and Dodson, 1963; Clarke et al., 1990; Omenda, 1998). These rocks occur from the surface down to a depth of about 500 m. Comendite is the dominant rock in this formation.

The youngest lava of the Upper Olkaria formation is the Ololbutot comendite, which has been dated at 180±50 years (Clarke et al., 1990). The vents for this young lava and associated pyroclastics were structurally controlled, with most of the centres occurring along N-S faults/fractures and a ring structure.

2.3 Tectonic setting of the Greater Olkaria volcanic complex

The geological structures of the Greater Olkaria volcanic complex are known to be the main controller of fluid movement and permeability properties in the geothermal reservoir. The geological structures in the GOVC are more prominent in the Olkaria East, Northeast and West fields but are elusive in the Olkaria Domes due to substantial cover of the surface geology by ashes, pumice and other pyroclastic deposits from recent volcanic eruptions (Odongo, 1993). However, through drilling, buried faults have been indicated in the Domes area. This has been demonstrated by cave-ins, loss of sample cuttings, drilling fluids, cement and occasionally the collapse of wells during drilling as evidenced by the recently drilled well OW-915B (KenGen, 2012).

The main structures controlling fluid movement within the GOVC are the O'l Njorowa gorge, the N-S, NW-SE, NNW-SSE, ENE-WSW faults and the ring structure (Figure 6). The NW-SE and WNW-ESE faults are thought to be the oldest and are associated with the development of the rift. The most prominent of these faults is the Gorge Farm fault, which bounds the geothermal fields in the northeast part and extends to the Olkaria Domes area. The most recent structures in the Olkaria volcanic complex are the N-S and NNE-SSW faults and are associated with the latest tectonic activities (Omenda, 1998). The Olkaria fracture and the Ololbutot fault zone are examples of these fault systems. According to Mungania (1999), the numerous phreatomagmatic craters located on the northern edge of the Olkaria Domes area were produced by magmatic explosions which occurred in submerged country. These craters form a row along which the extrapolated caldera rim trace passes. The dike swarms, well exposed in the O'l Njorowa gorge, trend in a north-northeasterly direction, further attesting to the recent reactivation of faults with that trend. The development of the O'l Njorowa gorge around 9000 years ago is believed to have been initiated by faulting along the trend of the gorge. Clarke et al. (1990) attributed the current steep walls and depth of the gorge to a catastrophic outflow of Lake Naivasha during its high stands. The O'l Njorowa gorge cuts the suggested ring structure from north to south.

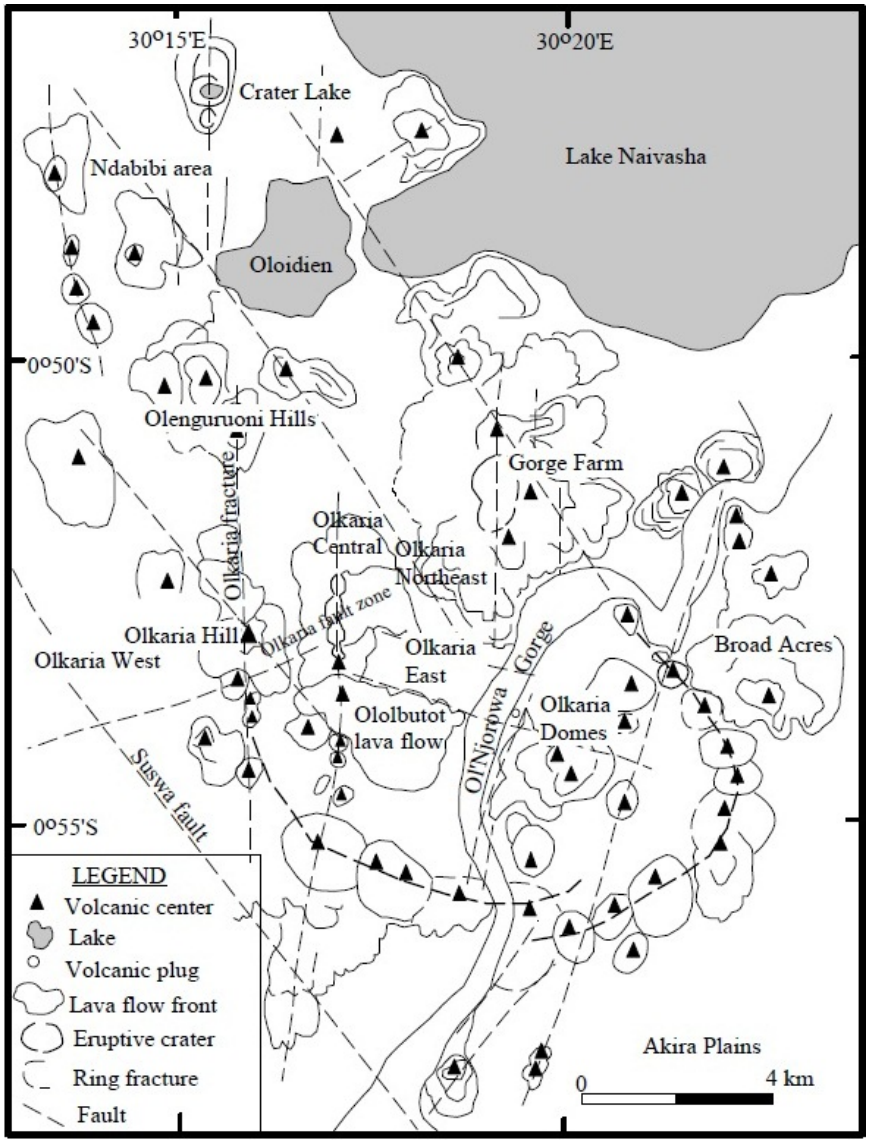

FIGURE 6: Structural map of the Greater Olkaria area (Omenda, 1998)

The ring structure in the Greater Olkaria volcanic complex is marked by the alignment of eruption centres over the southeast and the western boundaries of the area and is split into two: the inner and the outer ring. The ring of domes is thought to show the presence of a buried caldera that might have been produced by the magmatic stresses in the Olkaria magma chamber. The ring structure in the Olkaria area pre-dates the north-south tectonic trending pattern in the Rift Valley zone. The resulting caldera basin was formed by the explosive volcanic episodes and was then filled in with voluminous lava flows and pumiceous ashes from subsequent volcanic activities (Naylor, 1972). The heat source for the geothermal fluids in the area was, therefore, considered to be related to the devastated volcano (Omenda, 1998).

2.4 Geophysical setting

Several geophysical studies have been carried out in the Greater Olkaria geothermal area since the early seventies with varied levels of success and detail and continue to the present. The study methods employed encompass resistivity, magnetism, seismology and gravity (Mwangi, 1984). Resistivity studies based on a combined interpretation of transient electromagnetic (TEM), DC-Schlumberger, and magnetotelluric soundings within the area show that the low-resistivity anomalies are controlled by linear structures with NE-SW and NW-SE trends. The studies further attest that the geothermal resource is defined by low resistivity of 15 Ωm at 1000 m a.s.l. (Figure 7). The resistivity is generally lower in Olkaria West than in the eastern Olkaria fields (East and Northeast fields). This resistivity difference is a result of the differences in the geology from the surface to shallow depths.

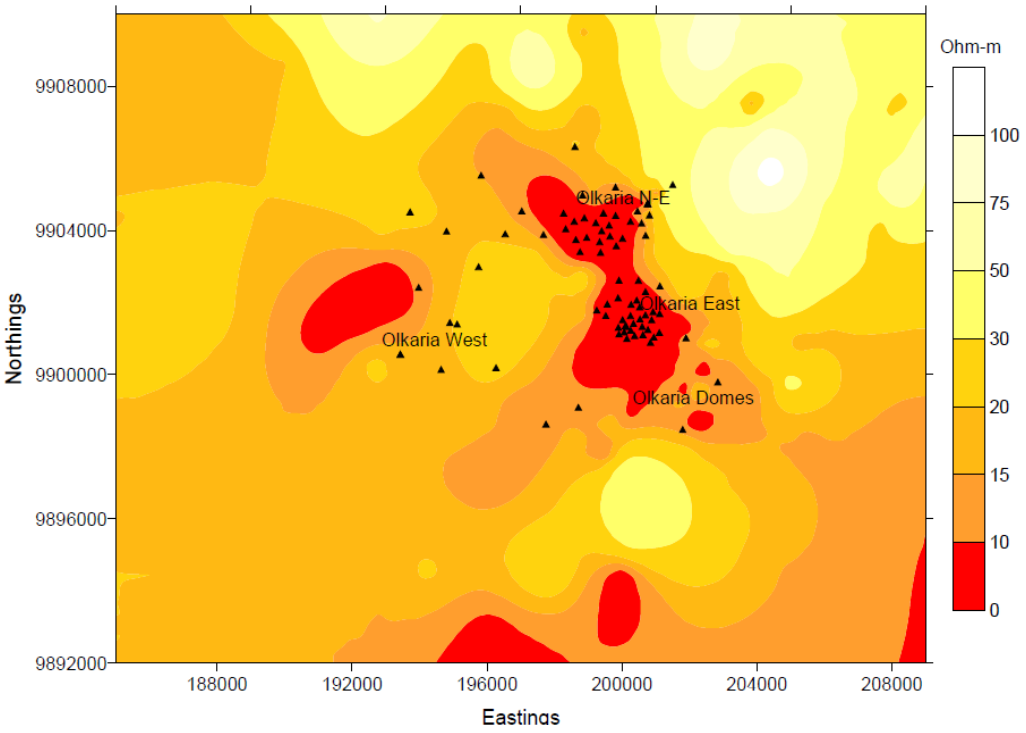

FIGURE 7: Resistivity distribution in greater Olkaria at 1400 m a.s.l. from TEM measurements (Mariita, 2009)

According to Muchemi (1999), the Olkaria West field is characterized by low-pH fluids, extensive alteration due to thick tuff strata and high permeability, consequently lower resistivity anomalies. In contrast, the relatively higher resistivities characterizing anomalies in the Olkaria eastern fields are due to the hosting of the reservoir within the flood trachytes.

The trachyte inhibits low susceptibility to alteration, except along secondary structures. The extreme low-resistivity anomaly near Olkaria Hill in the West production field was postulated by Mariita (2009) as the heat source for the Olkaria West geothermal field.

Interpretation of gravity data from the Greater Olkaria volcanic complex shows that a dense body occurs in the southern part between O'l Njorowa gorge and Suswa lineament. The Olkaria West, East and Northeast fields occur within gravity lows (Ndombi, 1981).

Micro-seismic monitoring of earthquakes within the Greater Olkaria area indicates that the area is characterized by relatively high-level micro-earthquake activity (Simiyu and Malin, 2000). Interpretation of S-wave attenuation data derived from this area has indicated a large volume of partially molten material below the Olkaria Domes, Northeast and West production fields, with other

smaller attenuating bodies, possibly indicating further undiscovered geothermal resources (West-JEC, 2009).

In the Olkaria Domes area, seismicity has shown the area to be a continuation of the Olkaria Northeast field along a major NW-SE linear structure. This area is characterized by both shallow and deep events that have been interpreted as volcano-tectonic and tectonic events (Simiyu and Keller, 1997).

In summary, the geophysical studies within the Greater Olkaria area have led to the following conclusions for the conceptual model of the Olkaria geothermal system (West-JEC, 2009):

- Three major sources appear to supply heat to the system, mainly inferred from S-wave attenuation data and partly supported by resistivity data. These are located beneath the West field, the Northeast field and the Domes area. They are possibly offshoots of a deeper lying magma chamber (Figure 8)
- The ring structure/fracture passing through the Domes field is likely a zone of permeability where up-flow occurs.
- There are indications of additional geothermal resources in the south-central and southwest Olkaria field (S-wave attenuation and resistivity), north of the Domes field and east of the Eastern field (S-wave attenuation), southeast of the Domes field (resistivity) and on the northeast edge of the Northeast fields (S-wave attenuation).

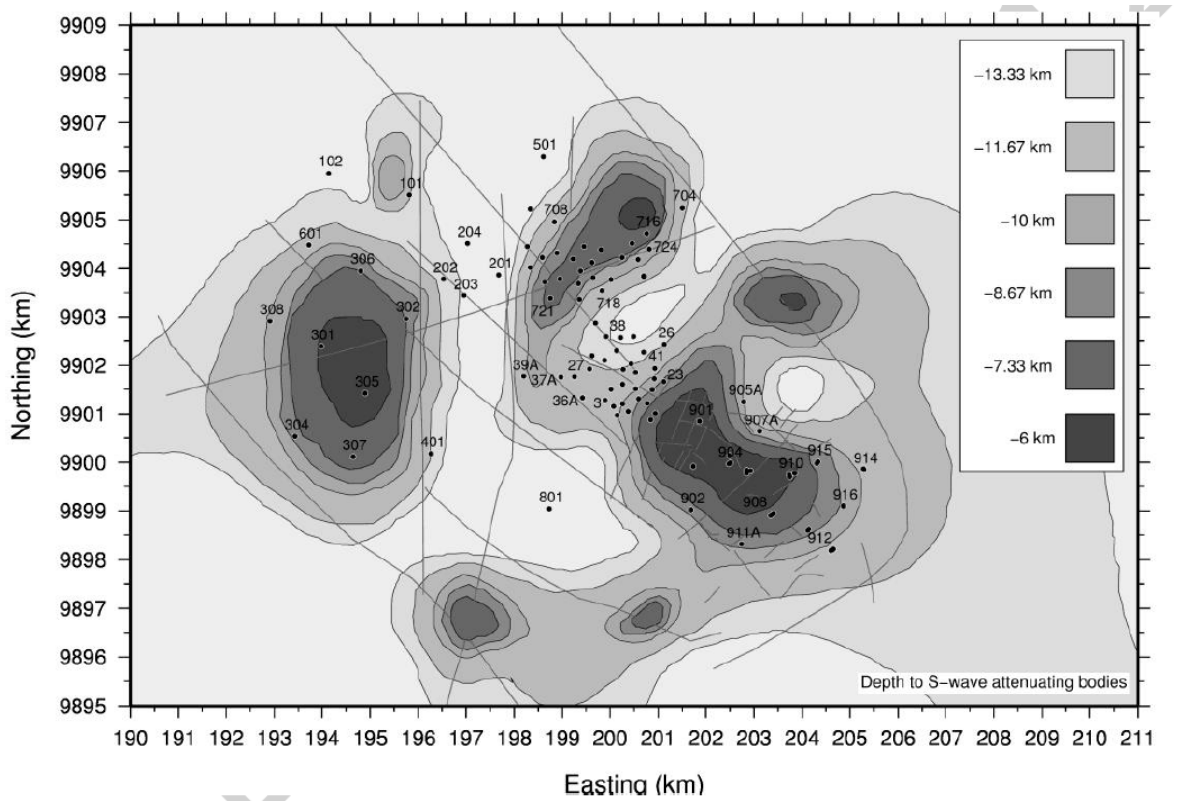

FIGURE 8: Contour map showing the tops of attenuating bodies beneath the Olkaria geothermal field (Simiyu, 1998)

2.5 Fluid chemistry of the Greater Olkaria fields

Detailed fluid chemistry studies have been carried out in the Olkaria fields over the past years as reported by earlier workers: Olkaria West (Muna, 1990; Wambugu, 1995); Olkaria Northeast (Wambugu, 1996); Olkaria East (Karingithi, 2000); Olkaria Domes (Karingithi, 1999). Fluid

chemistry data are essential information required for the characterization of geothermal fluids and the evaluation of the energy potentials of geothermal fields by geothermometry (Malimo, 2009). In addition, they provide a good indication for monitoring reservoir changes in response to production and also allow evaluation and avoidance of scaling problems in wells and surface pipelines.

The fluid chemistry in the Olkaria West field contrasts sharply with that in the eastern Olkaria fields. In the Olkaria West field, the discharge is distinctly highest in bicarbonates (10,000 ppm) but the chloride content is quite low (100-200 ppm), except in well OW-305. Comparatively, wells in the Olkaria East and Northeast fields tend to be high in chloride concentrations (300-600 ppm) and with similar bicarbonates-carbonates concentration of <1000 ppm (Wambugu, 1995).

The high bicarbonates concentration in the Olkaria West field is considered to be a consequence of CO_2 supply to the geothermal fluid and a subsequent reaction between the carbonic acid and mineral constituents of the rock which act like bases, thus converting some of the CO_2 to bicarbonate. The CO_2 source is considered to be predominantly from the magma heat source of the geothermal system although carbon present in the rock may contribute a little. Well OW-305 discharges water similar to wells in Olkaria East and Northeast fields. It is thought to be tapping the up-flow fluid from the Olkaria West field, while other wells are thought to discharge fluid which has been diluted by either steam condensate or shallow groundwater. The high chloride concentrations observed for the Olkaria East and Northeast fields could be the consequence of upflow of deep high-temperature geothermal fluid (Giggenbach, 1991), although progressive boiling by heat flow from the rock may also contribute in the Olkaria East field.

The diagram in Figure 9 shows that wells in the Olkaria West field discharge sodium-bicarbonate type water, while wells in Olkaria East and Northeast fields discharge sodium-chloride type water. Wells in Olkaria Central field discharge a mixture of the chloride and bicarbonate end member water as do wells in the Olkaria Domes area (Karingithi, 2000).

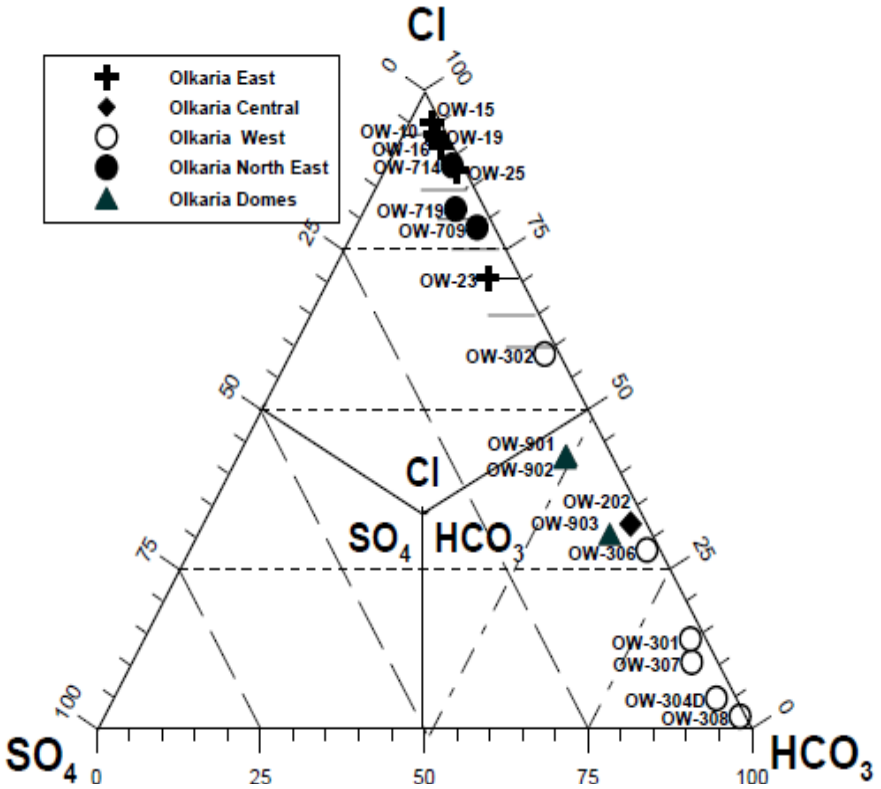

FIGURE 9: Cl-SO_4-HCO_3 diagram for selected Olkaria geothermal well samples (Karingithi, 2000)

3. DRILLING OF WELL OW-37A

Well OW-37A is located in the Olkaria East production field at 37N 9901748 N, UTM 18975.49, and at an elevation of 2017 m. It is a directional well drilled to a depth of 2848 m in N315°E direction. The surface, anchor and production casings were set at 52, 286 and 746 m, respectively. The aim of drilling this well was to gather steam for the 140 MWe Olkaria I power plant units 4 and 5, and to confirm the extent of the resource northwest of the Olkaria East production field. Figure 10 shows the drilling programme for the well.

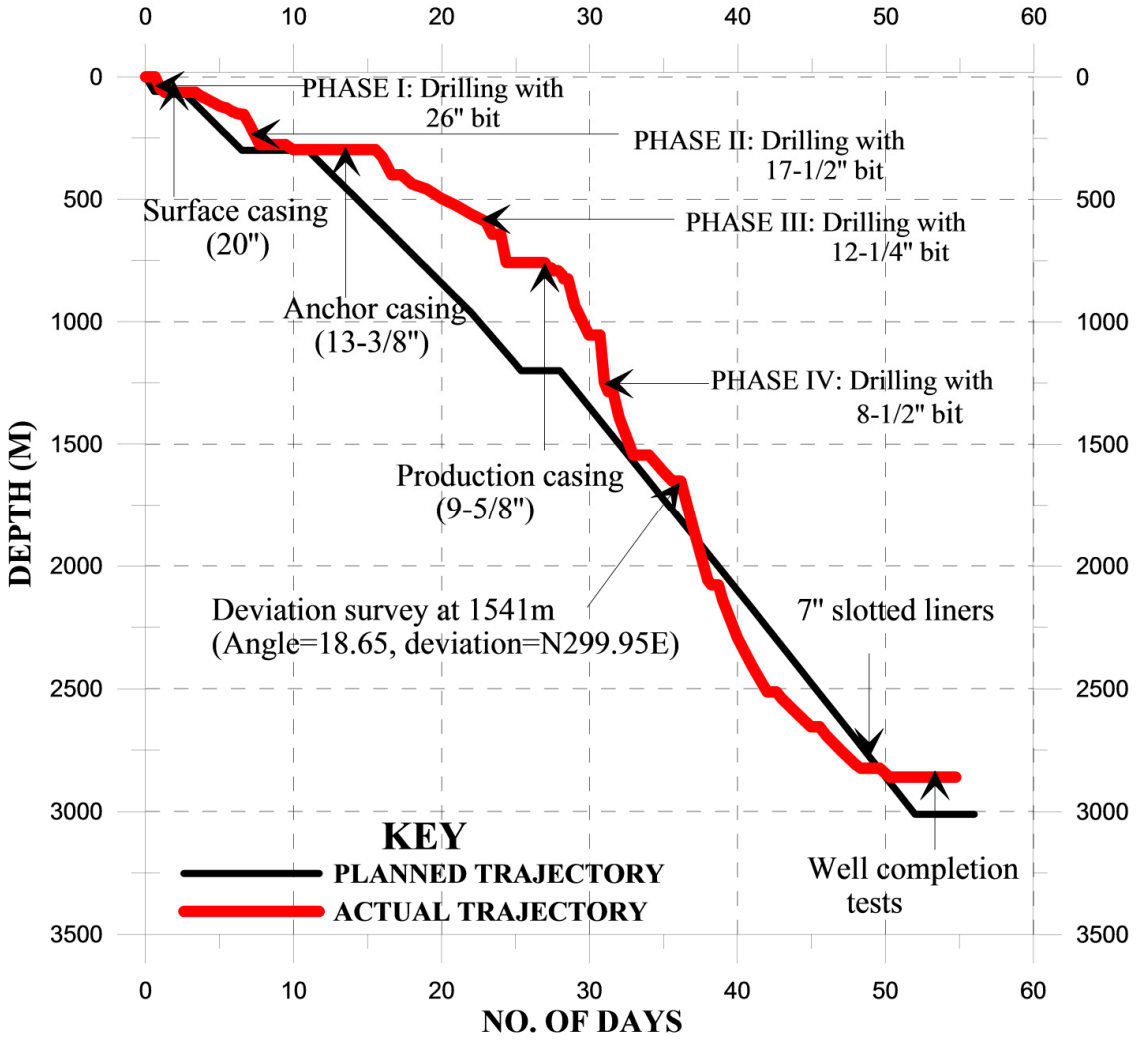

FIGURE 10: Drilling programme for well OW-37A (KenGen, unpublished data)

The well was spudded in on Tuesday, 31st March, 2009 at 15:40 hours using drill rig GWDC-116 and drilling was carried out in four phases, illustrated in Table 1.

TABLE 1: Drilling and casing design for well OW-37A

Drill rig	Stage	Drilling bit (")	Depth(m)		Casing	
			From	To	(“)	Type
GW-116	Pre drilling	26	0	52	20	Surface casing
GW-116	1st stage	17½	52	286	13⅜	Anchor casing
GW-116	2nd stage	12¼	286	746	9⅝	Production casing
GW-116	3rd stage	8½	746	2850	7	Production section

Phase I: Pre drilling was done using a 26" inch drill bit from the surface to 52 m with mud for a 20" casing. Good circulation returns were received on the surface between 0 and 22 m. However, between 22 and 52 m drilling continued blindly with mud as this section was dominated by total circulation loss. Surface casing of 20" size was run and a cement job was carried out using 2.137 tons of cement for both the primary cementing and the first backfill. On Friday, the 3rd April, 2009 at 03:40, the casing was cut, the flange was welded and the BOP's was nippled up and the pressure was tested. This phase lasted for 4 days.

Phase II: Drilling resumed for phase II on 3rd April, 2009 at 08:00 using a 17½" bit and mud as the drilling fluid. Drilling continued smoothly from 52 down to 106 m with good circulation returns. Total circulation loss was encountered between 106 and 116 m before drilling was halted on 5th April, at 08:40 to pave the way for the repair of a leaking wash pipe. At 10:02 drilling resumed using water between 116 and 142 m on a fairly hard and resilient formation in an attempt to regain circulation returns. On 6th April, at 09:17 drilling was once again halted to change the Bottom Hole Assembly (BHA). Running in hole of a new BHA was completed at 12:00 after which reaming of the hole began from 130 m to the bottom. Thereafter, drilling continued normally from 142 to 160 m with quite low rate of penetration (ROP) using aerated water and foam with partial to total circulation losses. From 160 to 266 m the formation became softer and ROP picked up. On Tuesday, 7th April at 16:20, the drill string got stuck, bringing the drilling operation to a standstill. As a result, the well was circulated using aerated water and foam in an attempt to free the stuck drill string. However, this proved futile until Friday, 10th April, when the string was successfully freed and immediately embarked on pulling out of hole (POOH) to inspect the BHA.

The hole was reamed to the bottom and drilling continued up to 286 m with good to partial circulation returns. The casing depth (286 m) was attained on the same day and a wiper trip was conducted prior to running in hole (RIH) of the 13⅜" anchor casing. RIH of the 13⅜" casing began on Saturday, the 11th of April at 04:30 but at midday an obstruction was encountered, hence POOH of the casings was conducted to ream the hole. On Sunday, the 12th of April at 20:00, the casings were successfully RIH. Cementing was done with primary cementing and five backfills, using a total of 73.28 tons of neat cement. This phase was completed in 13 days.

Phase III: Drilling for phase *III* began on Thursday, the 16th of April at 13:00 using water and foam. This was after the Bow-Out Preventer (BOP) stack was set up and a pressure test was done where all seals were found to be holding. Drilling of this phase continued smoothly with a total loss of returns between 286 and 298 m after which full circulation returns were regained to 320 m. At 00:45 drilling was stopped and the drilling crew immediately embarked on POOH to change the BHA, which lasted till 04:00, when RIH with the new BHA was completed. Reaming of the hole followed until 08:00. Normal drilling resumed on Friday, the 17th of April to 388 m in a fairly hard formation with moderate to low ROP with partial to full circulation returns realized. At 21:29 it was decided to circulate and clean the hole in readiness to POOH to install the mud motor which lasted until 04:30. Subsequently, reaming and circulating the hole were accomplished prior to continuing with the drilling. Drilling was continued in a hard formation from 388 to 394 m where a deviation survey was conducted. The inclination was measured at 3.8° at 394 m. Drilling continued to 588 m on a hard formation with low ROP with good circulation returns, where it was again decided to stop drilling in order to POOH to uninstall the mud motor and change the bit as well. Prior to POOH, another deviation survey was conducted and inclination was measured at 17.17°. RIH with the new bit began at 11:00 on Friday, 24th April. Drilling continued to 746 m, the casing depth on a soft formation with high ROP and good circulation returns except for a few intervals, where there were sporadic circulation losses. On Saturday, 25th April, a final deviation survey was conducted at 08:30 prior to POOH to RIH 9⅝" casings. The inclination was measured at 15.24° and POOH commenced immediately. RIH of the 9⅝" began at 20:00. Cementing began on Sunday, 26th April at 04:00 involving primary cementing and two backfills using a total of 51.59 tons of neat cement. This phase was completed in 11 days.

Phase IV: Drilling began on Monday, the 27th of April at 23:30 using aerated water and foam on a soft formation with good circulation returns. On Tuesday, the 28th April, drilling was temporarily halted at 03:00 in order to change the BHA after attaining 770 m. POOH for BHA change began at 03:15 and at 05:30, commenced RIH with the new BHA. Normal drilling was resumed at 10:00 with a total loss of returns. POOH at 12:15 was conducted to change the stabilizer and begin RIH with the new stabilizer at 15:00. Drilling resumed smoothly at 21:00 from 778 to 1102 m on a soft- to medium-hard formation with good circulation returns except for a few intervals where minor losses were encountered. Between 1102 and 1172 m there was total circulation loss. Full circulation was regained from 1172 to 1246 m after which a total loss was encountered to 1476 m. On Sunday, the 3rd May, drilling was stopped at 21:30 to inspect the BHA. POOH to change the BHA commenced at 22:00 and began RIH with the new BHA at 03:00. Drilling of the formation was resumed from 1532 to 2390 m with a total loss of returns except for some minor intervals where good to partial circulation returns were encountered. From 2390 to 2850 m, a total loss of returns was encountered.

On Thursday, the 21st May at 06:40 a final deviation survey was conducted prior to POOH to RIH the 7" slotted liners. The inclination was measured at 21.75° with a direction of N335.6°W. At 09:15 POOH began to the shoe to RIH the 7" slotted liner, which was successfully accomplished on Friday, the 22nd May at 13:00 hrs.

4. BOREHOLE SAMPLING AND ANALYTICAL METHODS

4.1 Sampling

Cutting samples from well OW-37A were taken at 2 m intervals, except in cases where the sample was too little and unrepresentative and a 4 m sampling interval was used. Preliminary analysis of the drill cuttings was done at the rig site with the aid of a binocular microscope. Specimen samples which were representative of the lithologic units penetrated were selected for detailed laboratory analysis of hydrothermal alteration minerals as well as for fluid inclusion studies. No cores were cut in well OW-37A; consequently all the descriptions and interpretations are based on the analysis of the drill cuttings.

Normally, the problem with analysing drill cuttings, as envisaged in well OW-37A, is that the rock chippings in some of the samples are very fine, often smaller than the crystals, thus making it difficult to conclusively identify some lithologic units. In addition, when the soft portions of the hydrothermally altered rock are ground during drilling, only the harder components reach the surface, hence less representative of the rock unit drilled through. Another common problem is the mixing of cuttings as a result of cave-ins, thus the need to carry out geosweeps where mixing of cuttings is suspected. Also, mixing of cuttings could be a result of travel time in very turbulent conditions.

4.2 Analytical methods

Four analytical methods were employed during sample analyses for well OW-37A. These encompass: binocular analysis, petrographic microscope analysis, X-ray diffractometer analysis and a fluid inclusion analysis, discussed as follows.

4.2.1 Binocular microscope analysis

Binocular analysis of the rock cuttings was done at the rig using a binocular microscope. Samples were scooped using Petri dishes and washed with clean water to remove dust and impurities. Wetting of the cuttings is essential to enhance the visibility of the samples and obscure features such as finely disseminated sulphides, e.g. pyrite. The sample is then placed on the mounting stage of the binocular

microscope and the crucial features noted, including the colour of the cuttings, rock fabrics, rock type(s), grain size, original mineralogy, alteration mineralogy and intensity, and finally vein and vesicle infillings.

4.2.2 Petrographic microscope analysis

The petrographic microscope is used to confirm the rock type(s) and alteration minerals, additional alteration minerals not discernible under the binocular microscope, and to study the mineralogical evolutionary sequence of the alteration minerals. Representative samples from all the lithologic units encountered in well OW-37A were selected and a total of thirty thin sections were prepared for petrographic analysis. The thin sections were analysed using a Leitz Wetzlar petrographic microscope.

4.2.3 X-ray diffractometer analysis

The X-ray diffractometer analysis is used to identify individual minerals present in rock cuttings, particularly clays and zeolites. A total of fifty-five samples were selected and analysed for clays. The < 2 microns fractions were prepared for X-ray diffraction by crushing the rock into fine powder and dissolving it in a test tube half full of distilled water.

The test tube is shaken and then left in a rack so that the <2 microns phyllosilicates are left in suspension. A few drops are placed on marked glass slides and left to dry so that the sample can be run using the XRD machine. A Shimadzu 6000 diffractometer, with CuKα radiation (at 40 kV and 50 mA), automatic divergence slit, fine receiving slit, and graphite monochrometer were used for the analyses. Count data were collected from 2°-35° at intervals of 0.02°, 2θ for a time of 1 second. The clay results are tabulated in Appendix I.

4.2.4 Fluid inclusion analysis

Fluid inclusions are fluid filled vacuoles sealed within minerals during growth or recrystallization. Fluid inclusion studies provide information about the densities and compositions of fluids trapped in minerals. The information can be used to estimate temperature and pressure conditions prevalent when the fluid was trapped. Double polished thick sections (approximately 70 microns) of cuttings from well OW-37A, which contained abundant quartz and calcite in veins, were prepared for fluid inclusion analysis. Primary fluid inclusions are formed during primary growth (crystallization) of a mineral and occur as isolated inclusions distributed within the crystal. On the other hand, secondary inclusions are incorporated into the host mineral during later processes (recrystallization) after the crystal has been formed. They are usually trapped along healed cracks. Upon cooling of the crystal, the fluid in the vacuole cools and contracts at a much faster rate than the solid and a vapour bubble will form. At ambient temperatures, all types of inclusions will contain a liquid aqueous solution and a gas bubble. This bubble forming process can be reversed to determine the temperature of mineral formation or the temperature of homogenization (T_h). The inclusion is heated until the fluid homogenizes in a single phase (i.e. the bubble disappears) and T_h is measured. The latter can then be used to deduce the temperature of the geothermal system at that time.

5. STRATIGRAPHY

The lithology of well OW-37A was established by binocular analysis of rock cuttings aided by petrography and XRD analysis. This was based on mineralogy, colour and texture. The litho-stratigraphy and drilling parameters of the well are shown in Figure 11. The numerous loss zones are also shown. The detailed stratigraphic description is given in Appendix III.

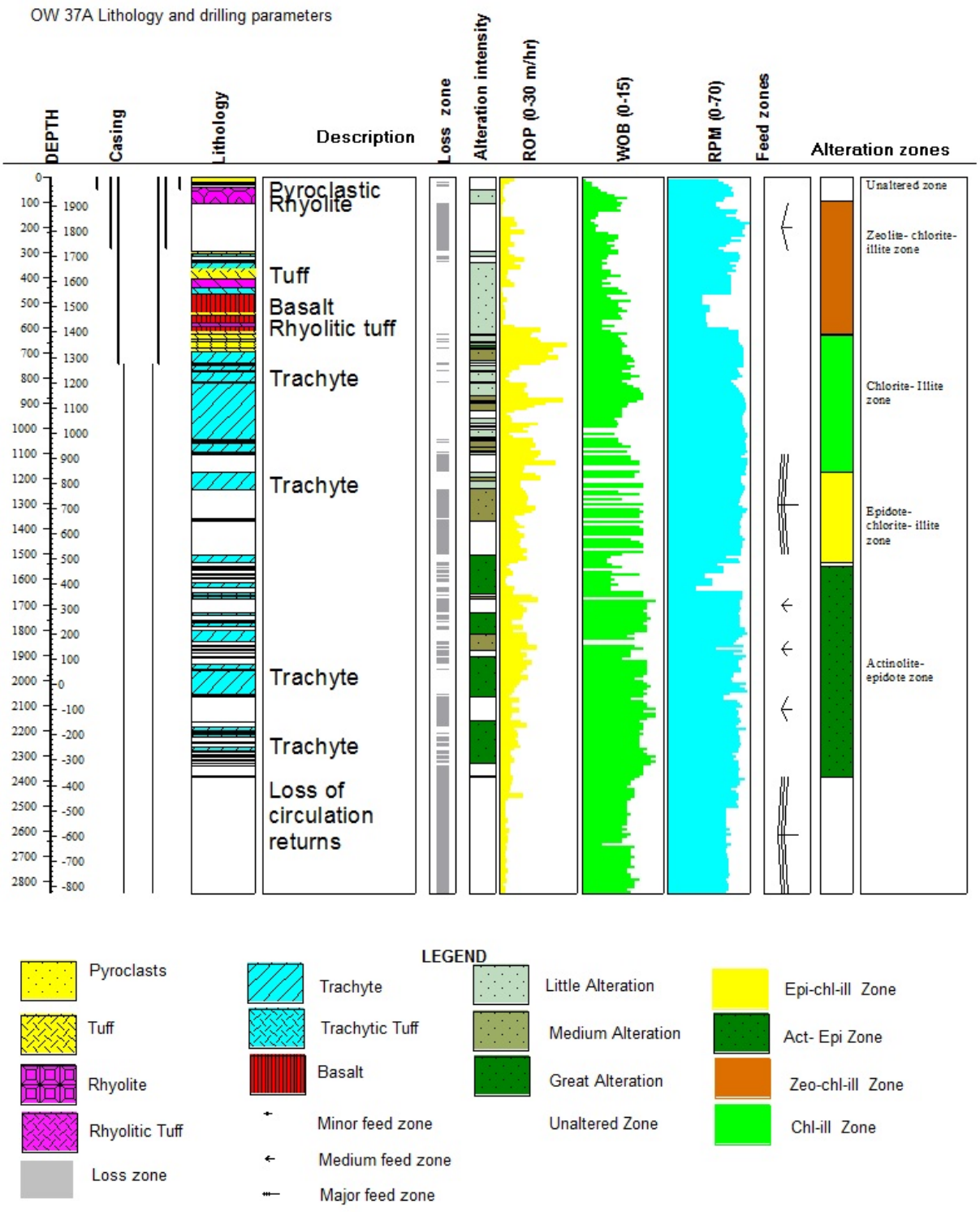

FIGURE 11: Lithology and drilling parameters of well OW-37A

Pyroclastics (0-60 m)

The top zone of this well is composed of brownish yellow, fine-grained, unconsolidated pyroclastics, mainly a mixture of volcanic glass, tuff and pumice fragments. Due to interactions with surface water and gases, the zone is highly oxidized.

Rhyolite (60-304 m)
Rhyolite is noted at 60-106 and 298-304 m. The formation is light grey, highly felsic and occurs as fine-grained phyric rock with sub-hedral to euhedral phenocrysts of quartz and sanidine. It shows slight oxidation with tinges of iron oxides.

Tuff (304-468 m)
Varieties of tuff, differing in colour, mineral composition and texture are noted ranging from 304-752 m as discussed below:

Acidic tuff is noted between 304-408 and 616-696 m. At 304-408 m the formation is light grey in colour, fine grained and highly fractured. Some grains appear vesicular and the formation also appears layered. Veinlets infilled with illite and pyrite are noted. The formation is slightly altered to chlorite, pyrite and illite.

At 616-696 m the tuff in this zone is light grey in colour, fine grained moderately porphyritic with sanidine phenocrysts. Vesicles infilled with illite, chlorite and calcite are noted as well as veins infilled with pyrite and illite. This zone is slightly altered.

Rhyolitic tuff occurs at 408-440 and 582-598 m. At 408-440 m, the rock is light grey to whitish, fine grained and phyric with phenocrysts of quartz and sanidine. It is highly vesicular with no infillings and highly fractured with pyrite and iron oxides infilling the veins. This zone is nearly fresh. At 582-598 m the formation is light grey, fine grained and vesicular with illite and chlorite, calcite and pyrite infilling veinlets and vesicles. The formation is slightly altered to illite, calcite, chlorite and pyrite.

Trachytic tuff. The formation occurs at 440-468 m and appears light grey, fine grained and slightly porphyritic with sanidine phenocrysts and secondary quartz crystals. The formation is slightly fractured and vesicular with euhedral pyrite cubes and secondary quartz infilling vesicles. Minor losses of circulation are noted in this zone and occasional brecciated fragments are noted in drill cuttings between 448-468 m.

Basalt (468-616 m)
Basalt occurs at 468-616 m being intercalated with tuff and rhyolitic tuff. The rock is grey to dark grey in colour, fine grained, mafic and moderately porphyritic with euhedral plagioclase phenocrysts and secondary quartz. It is fractured with quartz and pyrite vein fillings. Vesicles are predominantly filled with calcite.

Trachyte
Varieties of trachyte are noted differing in colour, mineral composition, texture and degree and mode of alteration. Trachyte occurs at 308-770 m where it is intercalated with basalt, tuff and scoria and at and 752-2384 m where it occurs with several losses of circulation returns in between. The different varieties of trachyte are discussed below.

308-364 m: The trachyte in this zone is grey, fine grained, highly porphyritic with sanidine phenocrysts and mafic specs of pyroxene. It is fractured with vein fillings and slightly oxidized. The formation also exhibits flow banding. The first appearance of secondary quartz is noted in this zone at 342 m.

696-740 m: Here the trachyte is grey to brown, fine-grained, slightly porphyritic lava with phenocrysts of sanidine. Pyrite cubes, unstable chlorite, illite and minor secondary quartz are noted. Generally this formation is slightly altered.

818-1062 m: Trachyte in this zone is grey to light brown, fine to medium grained, feldspar rich and moderately porphyritic with feldspar phenocrysts and specs of mafic minerals, mainly pyroxenes and amphiboles. The formation is highly fractured with illite and chlorite vein fillings. This zone is

moderately altered. However, it is intercalated with less altered grey-greenish, fine-grained slightly porphyritic lava with phenocrysts of feldspar and secondary quartz. Similar trachyte occurs at 1172-1184 and 1502-1532 m.

1062-1172 m: This is a less altered zone where the trachyte is grey to greenish, fine grained, slightly porphyritic with sanidine phenocrysts and slightly fractured with illite and chlorite vein fillings. This zone is moderately altered with well-formed pyrite cubes and secondary quartz. A similar trachytic formation occurs at 1184-1370 m. It is at this zone where epidote mineralisation is first noted at 1210 m and extends to 1370 m.

1548-1848 m: Trachyte in this zone is characterized as light grey, fine grained, highly porphyritic with phenocrysts of sanidine and exhibiting flow texture. The formation is slightly altered, some feldspar phenocrysts being replaced by adularia while others are slightly altered to pyrite, illite and chlorite. It is slightly fractured with illite and pyrite filling veins. A similar trachyte is found deeper at 2066-2216 m, however, the rock is moderately altered to illite, chlorite, pyrite and epidote.

1848-1894 m: Trachyte in this zone is grey in colour, cryptocrystalline and slightly fractured with pyrite, illite and chlorite vein fillings. The rock is slightly altered to actinolite, chlorite, illite and pyrite. Similar trachyte extends deeper at 1980-2066 m.

2216-2384 m: This zone is characterized by light grey, fine- to medium-grained, feldspar-rich trachyte with euhedral phenocrysts of sanidine. The formation is moderately altered to illite, actinolite, epidote, pyrite and secondary quartz. The rock is slightly fractured with illite and pyrite vein fillings.

6. HYDROTHERMAL ALTERATION AND TEMPERATURE DISTRIBUTION

Hydrothermal alteration is the process by which the mineralogy, chemistry and texture of a rock changes due to interaction with hot thermal fluids. The physical changes in the rock are in some incidences very conspicuous, especially where there is colour change (due to bleaching or otherwise), deposition of minerals, or development and obliteration of porosity and leaching. In all geothermal systems, proper understanding of the hydrothermal alteration is crucial as it is this information that gives the general picture of the geothermal system, its history and possibly its future. Most of the geothermal systems in the world display unique hydrothermal alteration characteristics based on several factors. The factors usually include temperature, pressure, rock type, permeability, fluid composition and the duration of fluid-rock interactions (Browne, 1978). However, according to Lagat (2004) temperature is one of the most significant factors in hydrothermal alteration because most of the chemical reactions require certain temperature conditions and minerals are thermodynamically stable at specific temperatures.

6.1 Alteration of primary minerals

Rock alteration simply means changing the mineralogy of the rock. Crystallization of primary minerals from magma is governed by the physico-chemical conditions under which the magma solidifies. The magmatic minerals are unstable at temperatures prevailing in geothermal systems, consequently getting replaced by more stable minerals during interactions with hydrothermal fluids. The instability of primary minerals in the geothermal environment is influenced by rock chemistry, permeability and the nature of the circulating hydrothermal fluids.

Broadly speaking, the order of alteration depends on the Bowen's reaction series (Figure 12) where the first mineral to be formed is the first to be altered, with quartz seldom being affected (Thomas, 2010). The alteration of primary minerals in well OW-37A conforms to the sequence observed in the Olkaria East field by Browne (1984a and b).

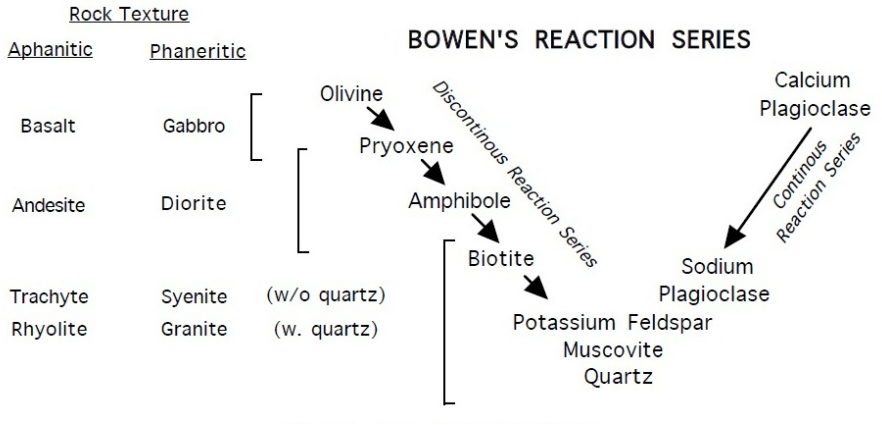

FIGURE 12: Bowen's reaction series (Thomas, 2010)

Volcanic glass, which is an important constituent of these rocks, is not strictly a mineral but it is relevant in this discussion owing to the fact that its replacement products bear relevance as hydrothermal minerals. The primary minerals and their alteration products in well OW-37A are summarized in Table 2. Also discussed in detail is the order of decreasing susceptibility of the primary minerals.

TABLE 2: Primary minerals and their alteration products in well OW-37A

Mineral susceptibility	Primary minerals	Alteration products
Most susceptible	Volcanic glass	Clays, calcite, quartz, chalcedony, zeolites
↓	Olivine	Clays, calcite, chlorite, actinolite
	Plagioclase	Calcite, clays, quartz, epidote, albite, wairakite,
	Sanidine	Albite, adularia, clays
	Pyroxenes	Clays, actinolite, chlorite,
Least susceptible	Opaques	Pyrite, hematite, sphene

Volcanic glass: This is the most affected and dominant primary mineral phase in the near surface rocks. It is noted in pyroclasts and rhyolites in the upper 106 m levels of the well, altering mainly to chalcedony, clays and zeolites and is also a calcite replacement. The formation of volcanic glass is attributed to rapid cooling of magma, hence not enough time for the magma to crystallize.
Olivine: Olivine is regarded as one of the minerals most susceptible to alteration due to its unstable nature, and it is the first constituent to be altered and replaced. The Bowen's reaction series attests to this fact since olivine is the first mineral to crystallize during formation of the rock (Figure 12). Olivine is noted in a basaltic unit between 470-482 m altering to clays and replaced by calcite. The mineral was not found in the trachytes and rhyolites.

Plagioclase: Plagioclase is the major rock forming mineral in basalts and is usually noted in the fine groundmass in rocks exhibiting porphyritic texture. The mineral is observed to be progressively altered as temperature increases and is finally replaced by albite. Other alteration products include calcite, wairakite, chlorite and epidote. In petrographic analysis, plagioclase is readily identified by the conspicuous polysynthetic twinning and low relief.

Sanidine: This is the dominant rock forming mineral in trachytic and rhyolitic formations and is noted to be replaced by adularia and clays from 632 m. However, with an increase in temperature, the mineral depicts a progressive alteration sequence. For example, from 1616 m, sanidines are noted to be completely replaced by albite (albitisation), signifying an increase in alteration. In petrographic

studies, sanidine is recognized by its colourless nature, low relief and is distinguished from the plagioclase by simple Carlsbad twinning.

Pyroxenes: Pyroxenes are more common in mafic rocks in comparison to silicic rocks. The prevalent pyroxene varieties encountered in this well are the clinopyroxenes. The latter occur in the matrix but are readily identifiable as mafic phenocrysts varying from augite, aegerine, and aegerine-augite. Generally, pyroxenes show some resistance to alteration but are noted to be progressively altered to actinolite from 1548 to 2848 m, the bottom of the well. Other alteration products include clays and chlorite. In thin section, pyroxenes are easily identified by two nearly perpendicular angle cleavage orientations with inclined (clinopyroxenes) or parallel (orthopyroxenes) extinction.

Opaques: The opaque minerals appear as mafic component in the rocks and show high resistance to alteration. However, with progressive temperature rise, the opaques alter to sphene, hematite and get replaced by pyrite. Fe-Ti oxide is the most common opaque mineral in basalts and trachytes. Magnetite is a common opaque mineral in fresh intrusive rocks.

6.2 Vein and vesicle fillings

Veins are micro-fractures that are filled up by either fluid or by the deposition of secondary minerals and can be due to primary jointing or later tectonic fractures. Vesicles, on the other hand, are pore spaces formed in the rock during an eruption as gas exsolves from magma. Despite the difference in structure, both are very important, not only as sources of permeability, but also as storage of fluid.

Hydrothermal alteration minerals, known to be very important geothermometers, are deposited within these structures and if carefully studied aid in the reconstruction of the palaeo-thermal history of a geothermal system. Basically, porosity and permeability are two of the principal factors that control the movement and storage of fluids in rocks and lead to the deposition of minerals either in veins or vesicles (Gebrehiwot, 2010).

In well OW-37A, the veins and vesicles fillings were identified under both the petrographic and binocular microscope. In the upper part of the well above 570 m, vesicles are mainly filled with calcite, quartz and clays. At greater depths, 616 m and below, vesicles were noted to be filled with wairakite (616 m), prehnite (696 m) and epidote (1210 m), indicating a considerable increase in temperature with depth. However, vesicles filled with actinolite were only noted under the petrographic microscope at 1780 m. The veins that were identified include quartz, pyrite, clays, wairakite and epidote.

6.3 Distribution of hydrothermal alteration minerals in OW 37A

In well OW-37A, hydrothermal alteration minerals appear to be both as replacement of the primary minerals, as well as fillings in vesicles, vugs and fractures. Figure 13 shows the distribution of alteration minerals in well OW-37A.

Zeolites are a group of authigenic minerals occurring at low-temperature geothermal conditions formed by the chemical reaction of the different types of volcanic rocks with alkaline groundwater. Different kinds of zeolites precipitate depending on physical and chemical properties. Below, the types of zeolites noted in well OW-37A are discussed.

Analcime occurs as colourless, equant crystals. This is a low-temperature zeolite whose occurrence indicates low temperature between 40 and 60°C. This mineral is quite rare in the well but was noted at 98-106 m.

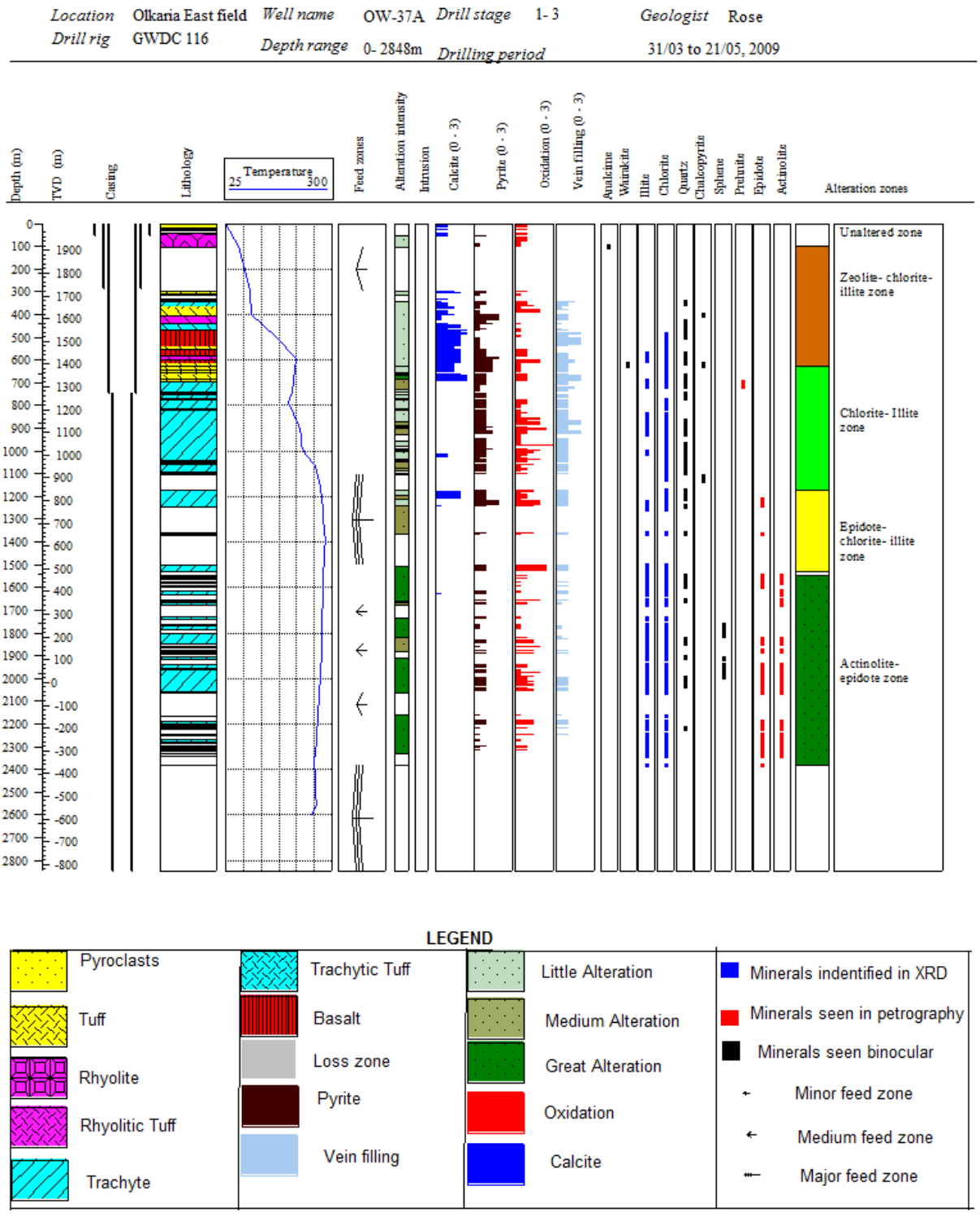

FIGURE 13: Alteration minerals and alteration zones for well OW-37A

Wairakite is a calcium-rich, high-temperature zeolite that occurs in the temperature range of 200-300°C. Deposition of wairakite started at 614 m in a basaltic formation. This is a rare mineral in this well.

Calcite. The formation of hydrothermal calcite relates to the movement of carbon dioxide in a geothermal system as governed by boiling, dilution, and condensation. The two principal calcite occurrences include replacement of rock forming minerals and volcanic glass and as platy crystals

infilling voids. Both are stable over a broad temperature range from 50 to 300°C (Thompson and Thompson, 1996).

In well OW-37A, the calcite occurs both as a replacement mineral and as a vein, vesicle and fracture filling. The first appearance of calcite is noted at 2-22 m and 26-32 m, infilling vesicles in pyroclasts (pumice and tuff fragments). Generally, calcite occurs from the surface to 1248 m, but is abundant at 300-700 m depth. Calcite occurs both as a vein filling and a vesicle filling. Crystal morphology of calcite is variable and ranges from individual thin-bladed crystals to needles. It appears as colourless or white massive crystals.

Pyrite forms brass yellow cubic crystals and has a strong metallic lustre. In well OW-37A, pyrite occurs both as massive and euhedral cubic crystals deposited in vesicles, fractures and veinlets as well as disseminations in the groundmass of the host rock. The occurrence of pyrite was observed between 52-2384 m. Abundant pyrite cubes were noted at 586-710, 948-1248 and at 1996-2204 m and its occurrence can be used to infer permeability or oxygen-rich fluids.

Epidote is a high-temperature alteration mineral whose first appearance indicates temperatures above 240°C. In well OW-37A, the first appearance of epidote is noted at 1172 m occurring as fine-grained aggregates and tabular or radiating crystals in vesicles. The mineral occurs sporadically at 1172-1596 and 2186-2384 m. In thin section, epidote was identified by its high relief, yellowish green colour with variable pleochroism from weak to moderate depending on the Fe-content of the mineral. The mineral is noted in association with pyrite, quartz, clays, and calcite.

Prehnite. In well OW-37A, prehnite was first identified at 696 m and occurs as white or greyish, with translucent spherical clusters of crystals with vitreous lustre. In thin section, the mineral has a moderate to rather strong birefringence and a bow-tie structure. Prehnite indicates temperatures of above 240°C and was noted in association with clays and quartz.

Hematite is an anhydrous iron oxide and was first noted at 1502 m depth in trachyte. The mineral occurs sporadically up to 1628 m. The mineral occurs with a red to reddish-brown colour and is formed by the oxidation of magnetite.

Chalcopyrite is a striking, bright yellow, metallic mineral that occurs in nearly all sulphide deposits. In this well, chalcopyrite occurs at 396 m and continues intermittently to 1070 m.

Fluorite is a low-temperature vein deposit and appears as translucent, well-formed coarse sized crystals disseminated in the rock matrix. Fluorite is one of the rare alteration minerals in this well; it was noted at 308-316 m.

Sphene is predominantly found as a replacement for ferromagnesian minerals. The mineral was first identified at 1762 m and extends to 1998 m depth. It is characterized by red to dark brown coloured crystals. In this well, sphene was found in association with chlorite, quartz and pyrite.

Actinolite is a higher geothermal temperature alteration mineral indicative of alteration temperatures above 280°C. In well OW-37A, actinolite's first appearance was noted at 1548 m but it also occurred at 2384 m.

Clays are water-rich phyllosilicates that form by hydrous alteration of primary silicate minerals and require the presence of water in liquid and/or vapour form. A number of environmental parameters control the composition, structure and morphology of clay minerals. These include temperature, fluid composition/amount, pH etc. (Ahmed, 2008). In the Greater Olkaria geothermal system, different types of clays are noted to occur at the surface where there is low-grade alteration, to the deeper zones where intense alteration is at play. The typical clay alteration products in well OW-37A consist of two types: chlorite and illite.

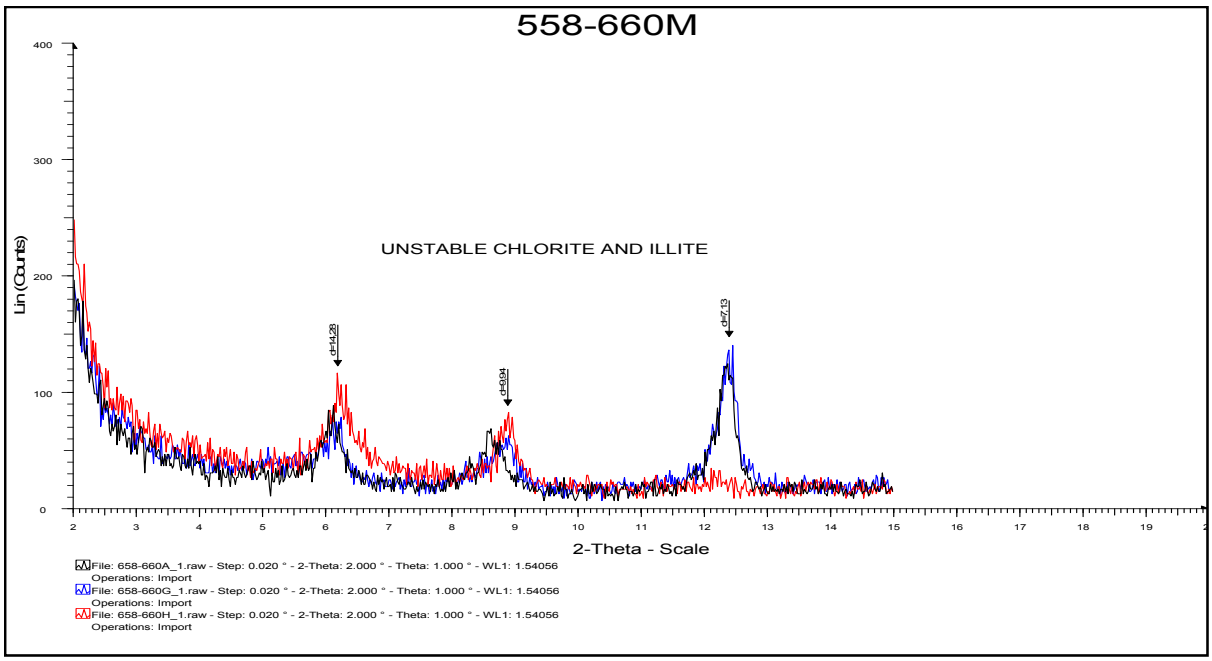

FIGURE 14: Diffractograms of clays showing unstable chlorite with illite

Chlorite occurs as green to dark green, coarse grained to fibrous, and represents temperatures of above 230°C. From the XRD analysis results, two kinds of chlorite can be deduced, including unstable and stable chlorite. The unstable chlorite is characterized by a d(001) peak at 14 Å for air dried, glycolated and heated samples, and a d(002) peak at 7 Å for air dried and glycolated samples but disappears completely when heated (Figure 14). In addition, unstable chlorite has typically a d(001) peak at 12.5 Å and a d(002) peak at 7 Å for air dried and glycolated samples with the heated peak collapsing as was common in this well.

In well OW-37A, the unstable chlorite first appears at 484 m and occurs periodically up to 1818 m. At 484-728 and 930-1818 m, unstable chlorite occurs in association with illite while between 784 and 836 m, the mineral is found exclusively. Stable chlorite, on the other hand, is characterized by a d(001) peak at 14 Å for air dried, glycolated and heated samples and also a d(002) peak at 7 Å for air dried, glycolated and heated samples as shown in Figure 15. The stable

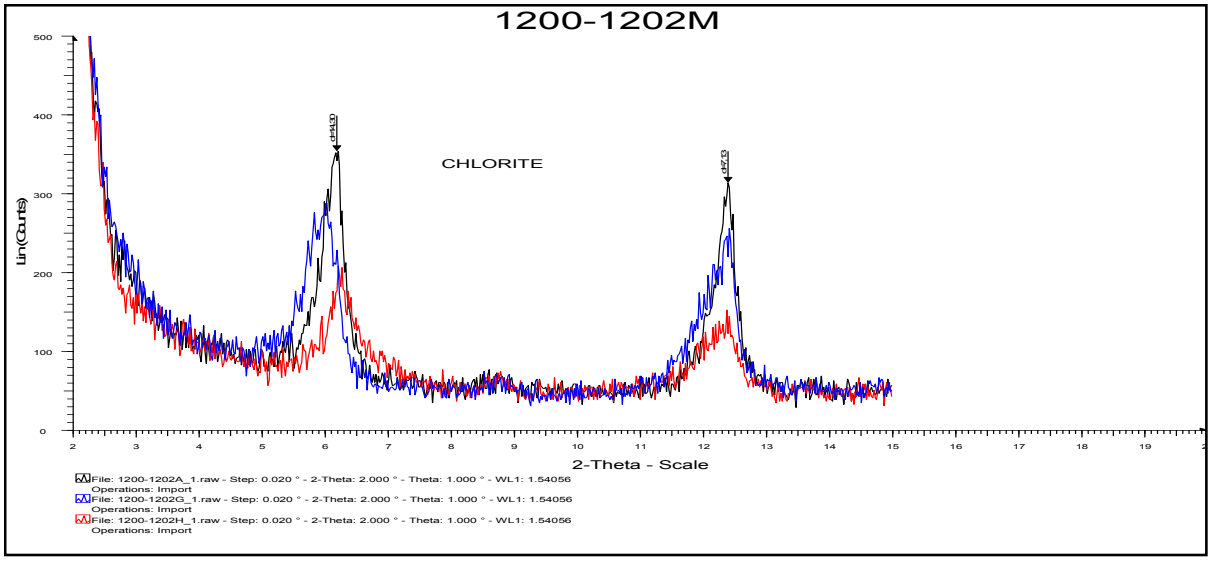

FIGURE 15: Diffractograms of clays showing stable chlorite peaks at 14 and 7 Å

chlorite is first noted at 664-682 m then disappears; the mineral reappears at 1862-2094 m both as chlorite-illite and exclusively as chlorite.

Illite is detected below 568 m in this well using XRD analysis and occurs sporadically to a depth of 2384 m. The mineral predominantly occurs as vein, vesicle and fracture fillings. In other cases, it is found as a replacement mineral in K-feldspars. According to XRD results, illite is characterized by a d(001) peak at 10 Å in the air dried, glycolated and heated samples. Illite is the most abundant clay mineral in well OW-37A. Occasionally, illite occurred solely. However, in most cases it was noted with either chlorite or unstable chlorite (Figure 14). A typical illite XRD pattern is shown in Figure 16.

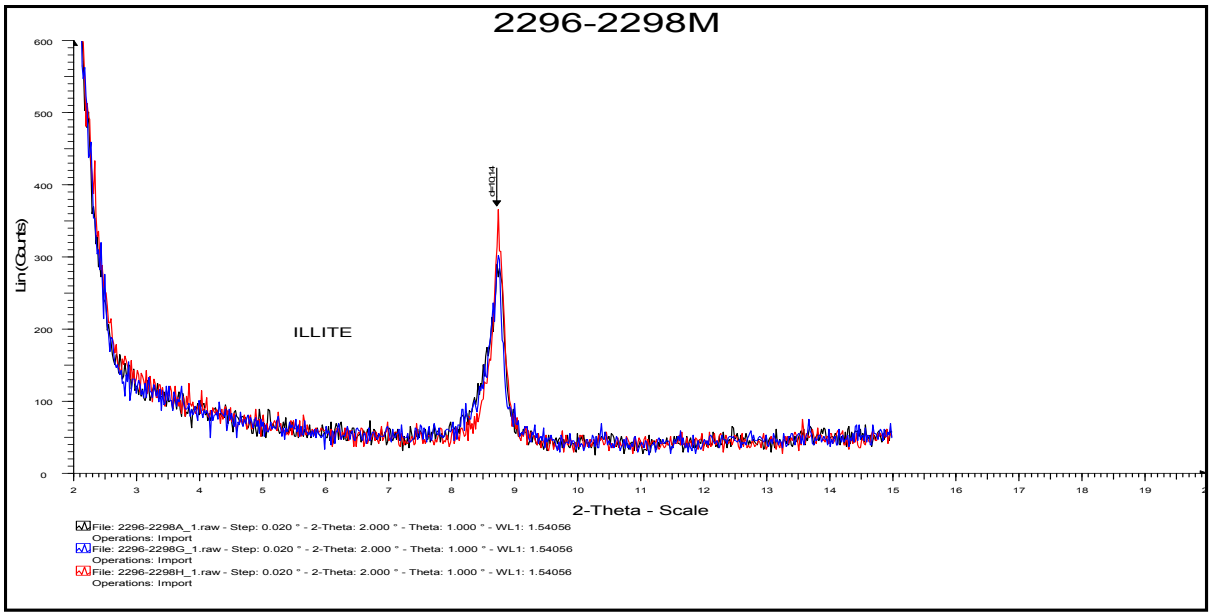

FIGURE 16: Diffractograms of clays showing illite peaks at around 10 Å

6.4 Mineral sequence and paragenesis

Paragenesis refers to the time successive order of deposition of a group of minerals in a fracture or a vesicle. A mineral deposition sequence/zoning is a powerful tool for geothermal sciences as it gives a historical account while at the same time deciphers the future of the geothermal system (Njue, 2010). A sequence in the mineralogical sense is a step wise or gradual progression of mineral deposition over time. Sequences typically occurring within veins and vesicles may be defined by visible boundaries and may display cross-cutting relationships. Mineral sequences occur in a manner such that the earliest mineral to be deposited is the one located on the outermost boundary of the vein or vesicle whilst the one succeeding it forms later and inward. Moreover, based on the principle of cross-cutting relationships, the veins that cut through others are considered younger in age. The depositional sequence in well OW-37A is marked by clay minerals, pyrite, calcite, quartz, and high-temperature alteration mineral assemblages commonly used as geothermometers. The sequence indicates the system is evolving from a cooler one to a hotter one. For example, in well OW-37A, wairakite is found to deposit first at 616 m followed by prehnite (696 m), epidote (1172 m) and actinolite (1548 m), a clear indication of temperature increase with depth. Table 3 summarises the depositional sequence in well OW-37A as observed using detailed binocular and petrographic analysis.

TABLE 3: Sequence of mineral deposition in well OW-37A

Depth (m)	Lithology	Alteration intensity	Alteration sequence Older → Younger
296	Rhyolite	Low	Fine-grained clay » pyrite
342	Trachyte	Low	Fine-grained clay » quartz » calcite
616	Tuff	Medium	Quartz » chlorite » wairakite
698	Trachyte	High	Quartz » chlorite » wairakite » prehnite
866	Trachyte	Medium	Chlorite » quartz
1014	Trachyte	Medium	Chlorite » quartz » calcite
1172	Trachyte	High	Quartz» chlorite » epidote
1548	Trachyte	High	Quartz » chlorite » epidote » actinolite
1654	Trachyte	High	Chlorite » epidote » actinolite
2186	Trachyte	High	Pyrite »chlorite » epidote » actinolite
2382	Trachyte	Medium	Chlorite » epidote » actinolite

6.5 Alteration mineral zonation

Unaltered zone (0-98 m): This zone extends from the surface to 98 m depth. It is composed of fresh rocks namely pyroclastics and rhyolite with no hydrothermal alteration except for reddish brown oxidation related to interactions with cold water.

Zeolite-chlorite–illite zone (98-626 m): This zone is characterized by an early appearance of analcime at 98 m and the later appearance of unstable chlorite with illite at 464 m. Wairakite, which is a higher-temperature zeolite, is first noted at 616 m. This indicates progressive heating towards the deeper zones of the well. Other minerals characterized by this zone include quartz, chalcedony, pyrite and calcite.

Chlorite-illite zone (630-1102 m): This zone is characterized by intense alteration to clays, notably illite and chlorite. The first appearance of prehnite was noted at 696 m. Other hydrothermal mineral assemblages in this zone include secondary quartz, pyrite, calcite and chalcopyrite.

Epidote-chlorite-illite zone (1172-1532 m): Chlorite and illite are identified as vein, vesicle and fracture fillings as well as replacements of primary minerals, mainly sanidine and amphiboles. The first appearance of epidote was noted at 1172 m and occurs sporadically throughout the zone. Other hydrothermal minerals noted in this zone, include secondary quartz, pyrite, chalcopyrite, calcite and hematite.

Actinolite-epidote zone (1550-2384 m): This zone is delineated by the first appearance of actinolite at 1550 m. Generally, this zone is characterized by high-temperature alteration mineral assemblages, including actinolite and epidote. Other alteration mineral assemblages include chlorite, illite, calcite, pyrite, secondary quartz, and hematite. The zone indicates alteration temperatures above 280°C.

6.6 Fluid inclusion geothermometry

Fluid inclusions are microscopic bubbles of liquid and gas formed during crystallisation or recrystallization of minerals. When hydrothermal minerals grow, or are recrystallized, in a fluid environment, tiny growth irregularities trap small amounts of the depositing fluid within the solid crystal (Mbia, 2010). Heating a fluid inclusion with vapour bubbles can be used to determine the temperature of homogenization during entrapment which then can be used to deduce the thermal history of the reservoir (Franzson, 2010).

In well OW-37A, three crystals, including two quartz crystals and one calcite crystal, were picked at a depth of 668-670 m and homogenization temperature measurements were carried out on a total of 52 inclusions. The homogenization fluid inclusion temperature (T_h) values at 668-670 m in well OW-37A ranged between 185 and 245°C in quartz and between 170 and 245°C for calcite. The formation temperature at this depth is 248°C. The lowest T_h value (185°C) in quartz veins from this well is 63°C below the calculated formation temperature and the highest value (245°C) is 3°C below the calculated formation temperature. The results are tabulated in Figures 17, 18, 19 and 20. According to Figure 17 most inclusions in quartz 1 crystal were formed between 230 and 245°C. Similarly, according to Figure 18, most fluid inclusions from a quartz 2 crystal were formed at 205-235°C. According to Figure 19, most fluid inclusions in the calcite 1 were formed at 205-250°C.

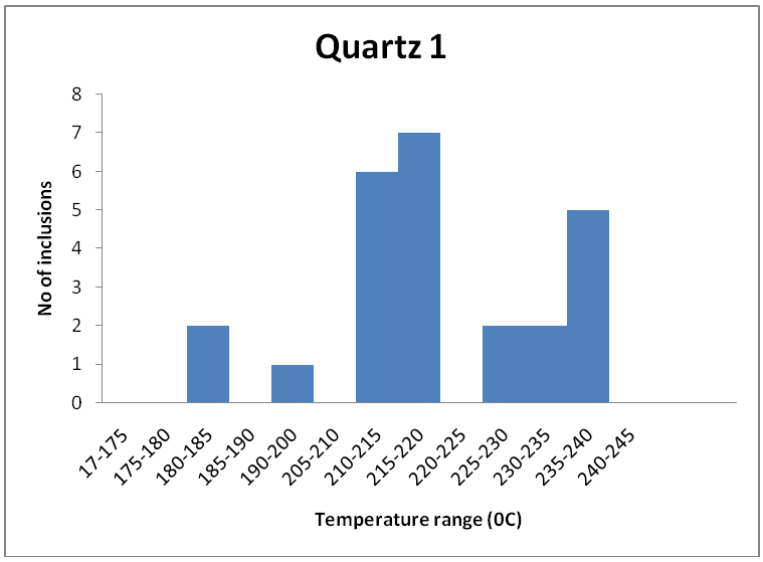

FIGURE 17: Quartz 1 fluid inclusion analysis results

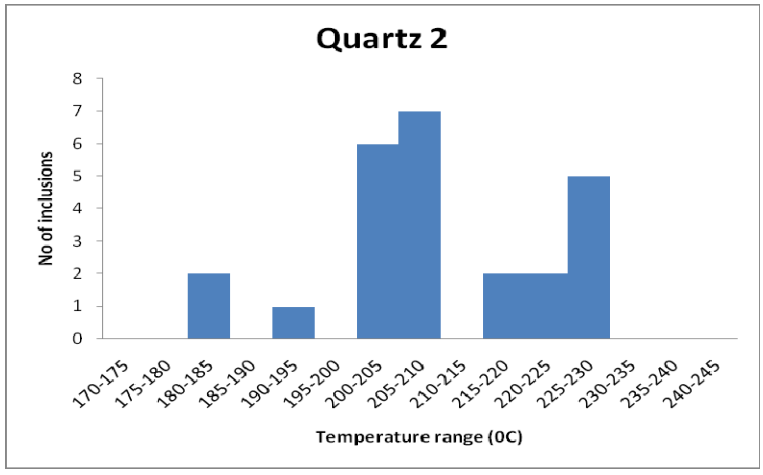

FIGURE 18: Quartz 2 fluid inclusion analysis results

On the other hand, calcite showed the lowest T_h value (170°C) to be 78°C below the formation temperature and the highest value (245°C) is 3°C below formation temperature. The average quartz value is 221°C, which is 17°C lower than the formation temperature. The average value for calcite is 212°C, which is 36°C below the formation temperature. From these measurements it can be deduced that some of the fluid inclusions in quartz and calcite crystals closely represent the current formation temperature conditions, i.e. the geothermal system has been more or less in a state of equilibrium since these inclusions were trapped.

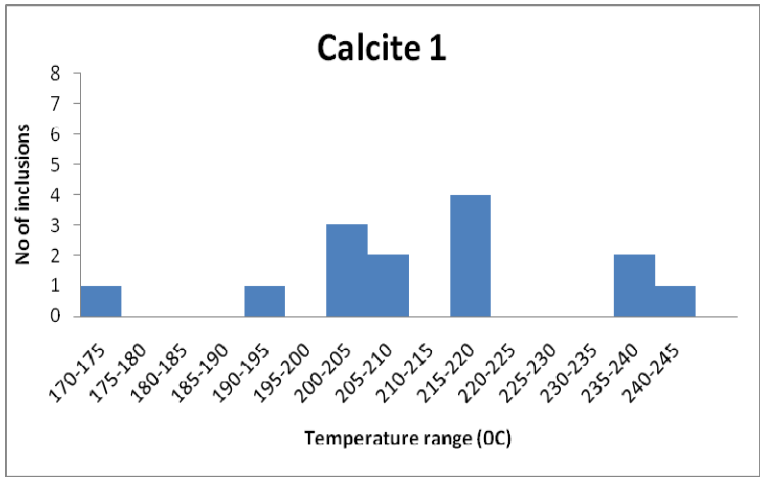

FIGURE 19: Calcite fluid inclusion analysis results

From the combined results for quartz and calcite homogenization temperature (Figure 20), it is clear that in well OW-37A there are

two temperature populations, one at 205-220°C and another at 230-245°C. Only very few inclusions were formed below 185°C.

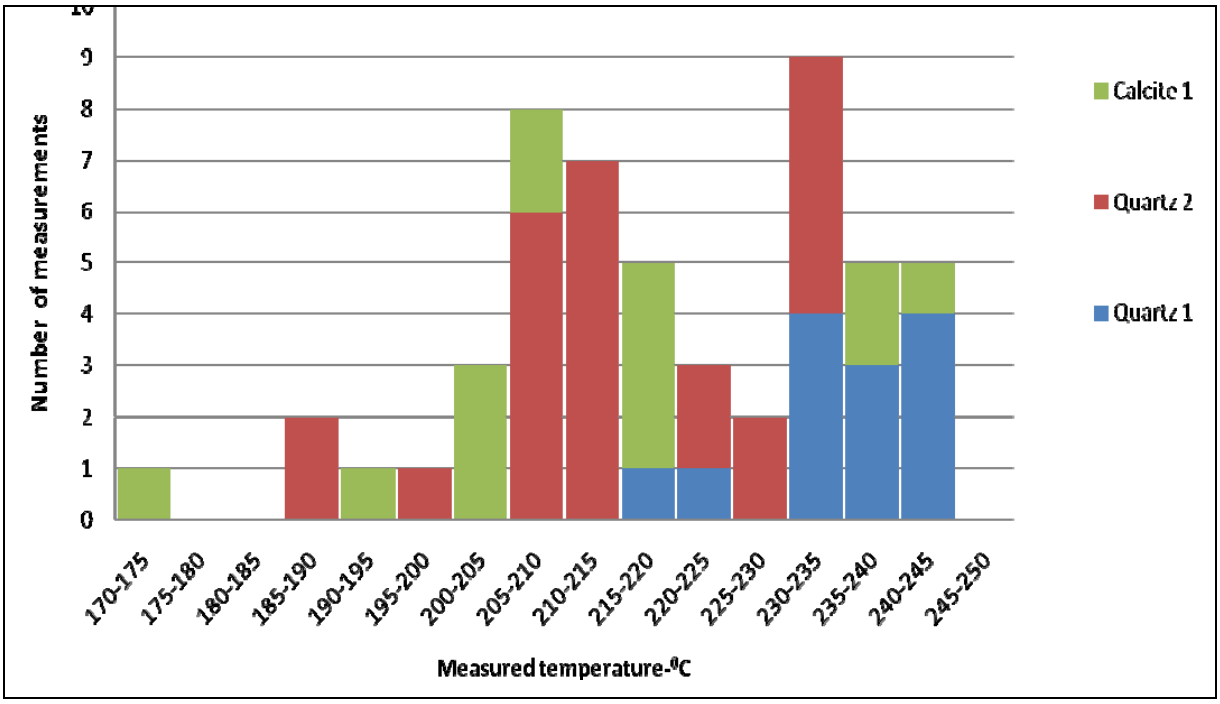

FIGURE 20: Combined fluid inclusion results

6.7 Measured, alteration and fluid inclusion homogenization temperatures

Fluid inclusion histograms were plotted with formation and alteration temperature curves to establish whether the geothermal system is heating, cooling or has been in a state of equilibrium over a period of time. Formation temperatures were calculated using a Horner plot based on the temperature profiles within 45 days of heating and during a well discharge test. The alteration temperature curve is based on the first appearance of alteration minerals observed using binocular and petrographic analysis; these minerals were used as geothermometers. Homogenization temperatures are the results of fluid inclusion analysis of quartz and calcite crystals.

A comparison of alteration and formation temperatures (Figure 21) shows higher alteration temperatures compared to formation temperatures from the top to 600 m depth. This indicates that the system has cooled down in this top zone. On the other hand, the system seems to be heating up from 600 m towards the deeper zones of the well where the formation temperature is higher than the alteration temperature. It is notable that the formation temperature curve nearly coincides with the measured temperature after 45 days of heating during the discharge test. This is because the formation temperatures indicate temperatures after the well has heated up and stabilized.

The fluid inclusion results indicate two temperature regimes with homogenization temperatures ranging between 205-220°C and 230-245°C, respectively. The latter formed at temperatures higher than the alteration temperatures but within the range of formation temperatures. This would indicate a younger group of inclusion. The 205-220°C regime (inclusions) is older since the temperatures are within the deduced alteration temperature (formed when the system was cooler) but much below the formation temperature.

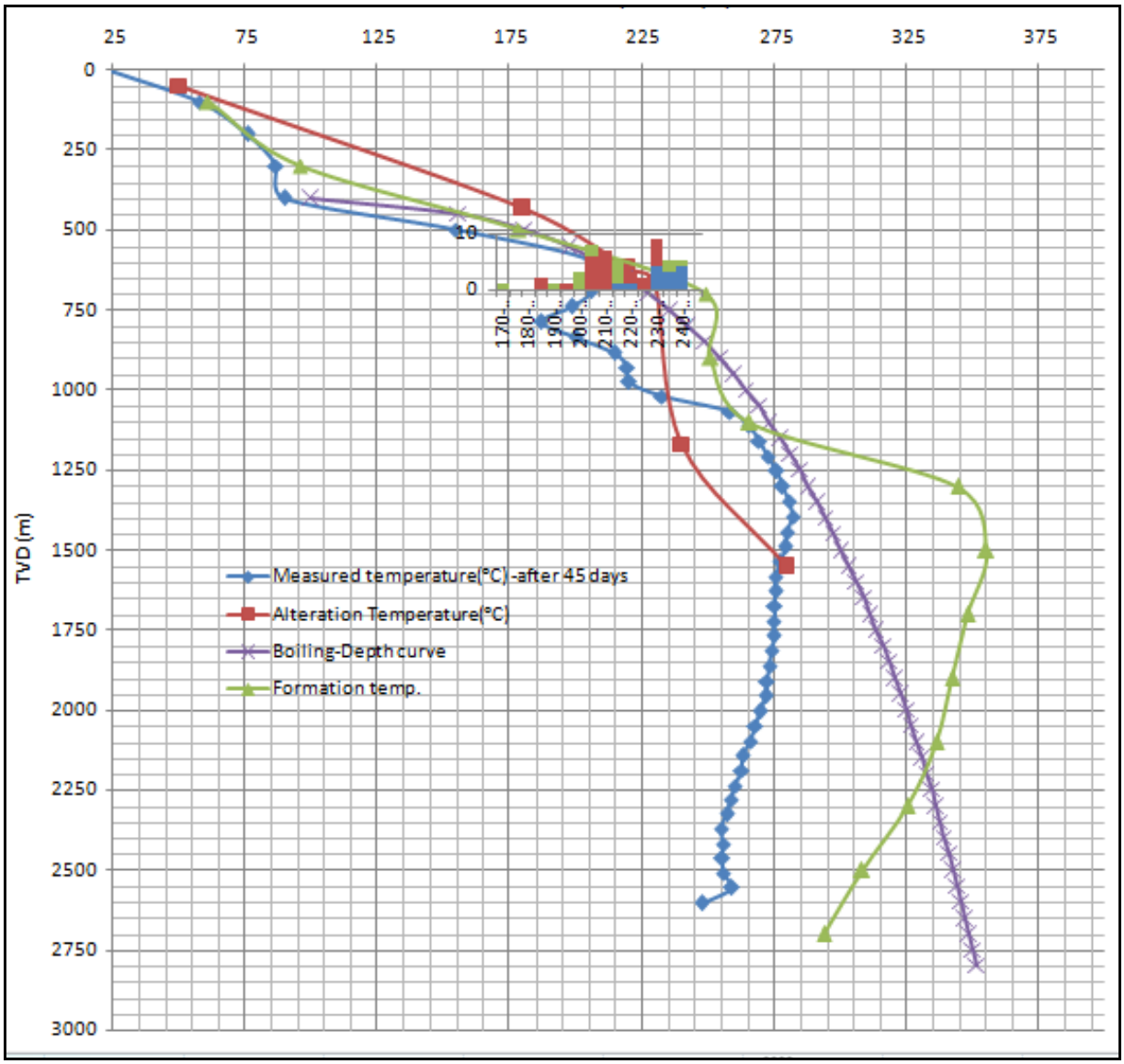

FIGURE 21: Comparison of homogenization, formation and alteration temperatures in well OW-37A

6.8 Aquifers / feed zones

An aquifer is a water-bearing rock, which is permeable and porous. Successful drilling in a prospective geothermal field is achieved if high-temperature permeable zones are intersected. The main sources of permeability in the Greater Olkaria volcanic complex are lithological contacts, intrusive boundaries and major faults and fractures. Koestono (2007) postulated that information on stand-pipe pressure and the rate of penetration during drilling contributes and aids in locating the feed points. For example, a high rate of penetration during drilling may be an indicator of aquifers, as does a drop in pipe pressure; a total loss of circulation in the zones may indicate the same.

Aquifers in well OW-37A were interpreted by circulation loss zones, hydrothermal alteration mineralogy patterns, and pressure-temperature recovery tests. The latter, other than serving as feed zone indicators are also used to evaluate formation temperatures.

Temperature and pressure log tools play an integral role in determining the reservoir characteristics in a well. In this well, step pumping using the temperature and pressure tool was conducted between 22nd March, 2009 and 26th June, 2009.

Temperature and pressure logs were collected during pre-injection and injection and recovery 14.5 hrs and 6, 17, 26, and 45 days after completion. The first pumping rate was set at 1000 lpm, and then subsequently increased to 1300 lpm, 1600 lpm and finally 1900 lpm. A plot of the downhole temperature and pressure logs was made to determine the water level, pivot point, feed zones, storativity, transmissivity and injectivity index.

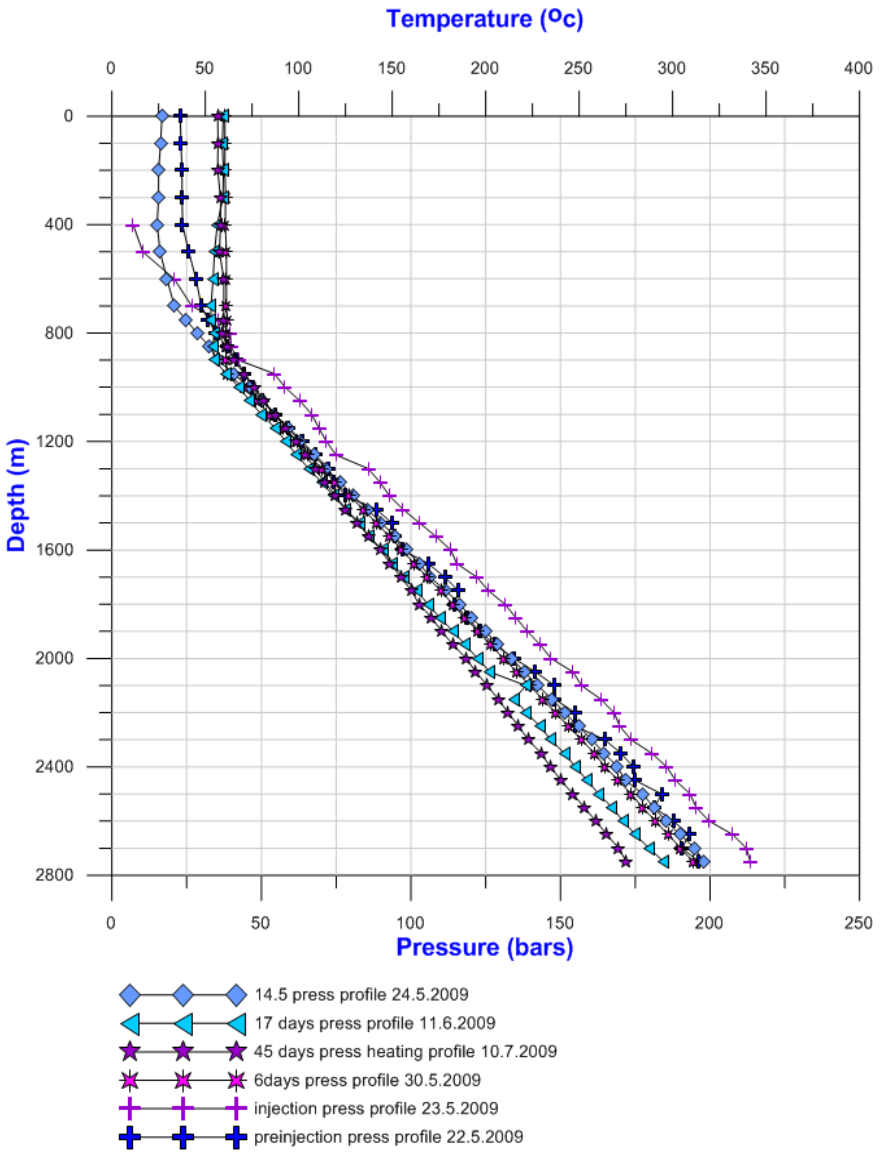

FIGURE 22: Downhole pressure profile for well OW-37A (KenGen 2009, unpublished)

Pressure logs in well OW-37A indicate the water level to occur at around 500 m while the pivot point is noted between 1100 and 1350 m (Figure 22).

From the temperature logs (Figure 23) the well appears to open down to the bottom. One large aquifer above the production part was inferred to occur between 106 and 298 m. This zone is marked by total circulation losses. Other small feed zones located above the production section were noted at 316-332, 336-342, 654-660, and 682-686 m. These are also characterized by circulation losses. Nonetheless, these aquifers were cased off since their temperatures were not high enough and would ultimately cool the well.

Aquifers within the production part can broadly be classified into small, medium or large depending on their sizes. The deflection in the temperature profile shows small to large peaks and indicates the relative size of the aquifer, ranging from small to large. Six small aquifers occur at 1848-1860, 1866-1878, 1882-1890, and 2280-2286 m. All these aquifers are marked by circulation losses. Seven medium aquifers were found at 1562-1578, 1632-1654, 1740-1762, 1914-1938, 2168-2186, 2224-2246, and 2480-2600 m.

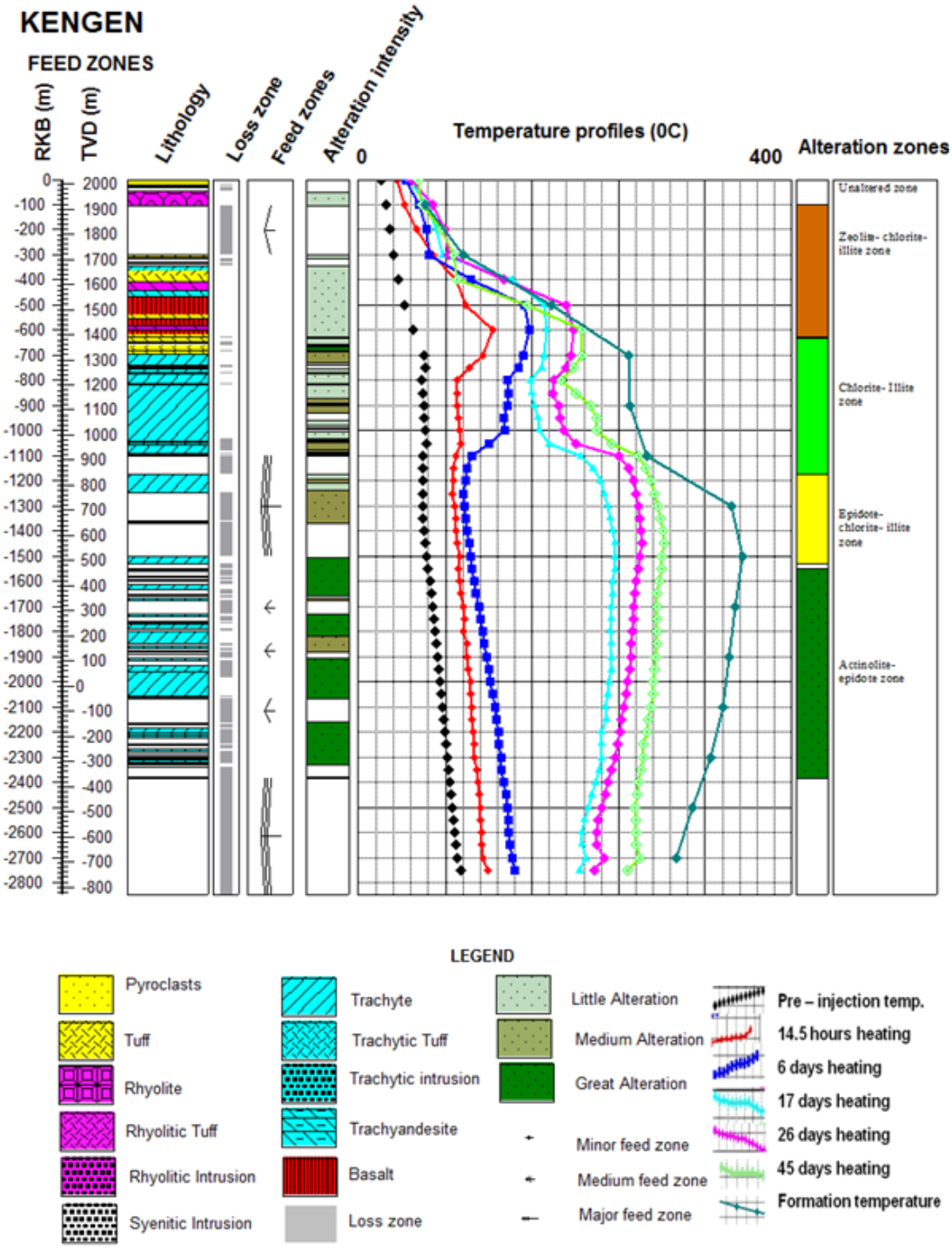

FIGURE 23: Well OW-37A feed zones and temperature profiles (KenGen 2009, unpublished)

Three major aquifers were noted, the first one occurring at 600 m. This zone is characterized by circulation losses and temperature recovery. The second major aquifer was noted at 860 to 1040 m and can be deduced from the temperature inversion appearing in the temperature log as well as via circulation losses. It appears that water is cross flowing between the aquifers in this zone. The third aquifer occurs between 1100 and 1480 m and is believed to be the one controlling the well. A distinct increase in temperature to about 265°C from 1100 m was evident from the temperature profile. This zone is also marked by circulation losses and fractured and highly altered trachyte. Further, the pressure profile indicates that the pivot point, which is considered an indicator of the best feed zone in

a well, falls within this zone. Table 4 shows the interpreted permeable zones based on evidence from geological and drilling observations.

TABLE 4: Interpreted permeable zones / aquifers based on geological observations

Depth (m)	Evidence from geological observations and drilling observations
106-298	Circulation losses
316-332	Circulation losses
336-342	Circulation losses
600	Circulation losses, fractured tuff and trachyte
860-1040	Circulation losses and fractured trachyte
1100-1480	Circulation losses and highly altered trachyte – also identified by a kink in temperature profiles.
1848-1860	Circulation losses
1866-1878	Circulation losses
1882-1890	Circulation losses
2224-2246	Circulation losses highly fractured trachyte
2480-2600	Circulation losses

7. LITHOSTRATIGRAPHIC CORRELATION OF WELLS OW-35 AND OW-37A

Wells OW-35 and OW-37A, drilled in the Olkaria East production field, encountered rock types at similar depths with slight differences apparently due to tectonic activity. Well OW-37A lies at an altitude of 2017 m a.s.l. while well OW-35 lies at 1960 m a.s.l. The basaltic lava flow which defines the caprock of the reservoir has been used as the marker horizon as it is widespread. Between wells OW-37A and OW-35 the basaltic lavas are encountered at 1549 and 1432 m a.s.l., respectively. This accounts for a 117 m lithological displacement to the east, inferred as a fault zone (Figure 24). According to Lagat's conceptual model of the Olkaria geothermal field (2004), a normal fault was found between these two wells, which coincide with our observation.

Epidote and actinolite are the two geothermometers used for correlation between wells OW-37A and OW-35 with their first appearances at 1172 and 678 m b.g.l. for the epidote, and at 1548 and 1624 m b.g.l. for the actinolite, respectively. Most alteration minerals and alteration zones were found at shallower levels in well OW-35 (Figure 24). This difference infers a possible cold down-low near well OW-37A and a hot upflow zone in the vicinity of well OW-35.

8. DISCUSSION AND CONCLUSIONS

8.1 Discussion

The stratigraphy of well OW-37A shows that unconsolidated pyroclastics make up the uppermost 60 m of the well. Rhyolite is noted at 60-106 and 298-304 m. The upper stratigraphic column of this well relates with the stratigraphic column of the Greater Olkaria volcanic complex as discussed by Shackleton (1986), Omenda (2000) and Odongo (1986). The surface and near surface geology is predominantly composed of pyroclastics and comenditic rhyolites of the upper Olkaria volcanics. In this well, pyroclastics and rhyolitic lavas dominate down to 304 m.

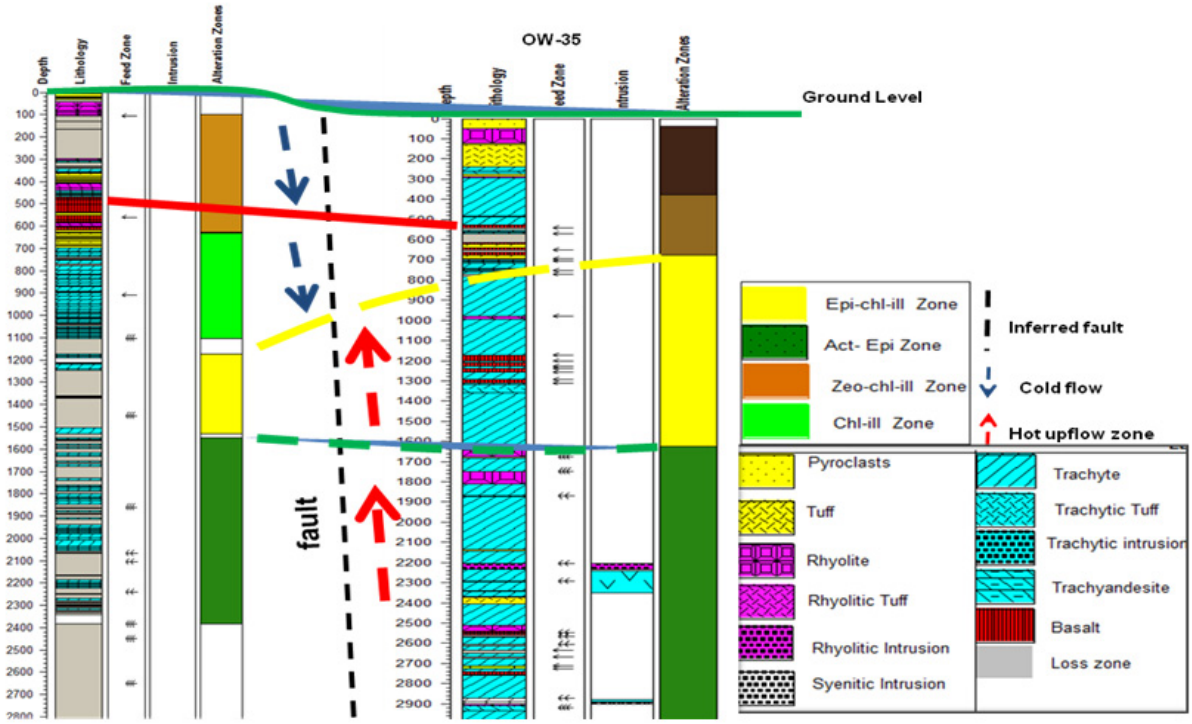

FIGURE 24: Lithostratigraphic correlation of wells OW-37A and OW-35

Three tuff varieties were noted in this well. The first variety is acidic tuff at 304-408 m; it is characterized by light grey colour, is aphanitic, highly fractured and appears laminated. The acidic tuff variety noted at 616-696 m is light grey in colour and phyric with feldspar phenocrysts. Rhyolitic tuff forms the second variety and occurs at 408-440 and 582-598 m. It varies in colour and texture from light grey to whitish and is porphyritic to non-porphyritic. The last variety of tuff is trachytic tuff. The latter occupies the depth between 440 and 468 m; colour varies from light grey to grey, and it is phyric with sanidine phenocrysts. Also, it is intercalated with brecciated fragments. The intermittent occurrence of tuff layers, intercalating with other lithological units may indicate that, in the past, this area experienced multiple episodes of eruptions. Each eruption began by the eruption of ash material, forming layers of tuff, followed by lava eruption overlaying the tuff layer.

The basaltic formation was first noted at 460 m and extends to 616 m, intercalated with tuffs and rhyolitic tuffs. The formation relates to the Olkaria basalt which is proposed to be the cap rock of the Olkaria geothermal system. It occurs with a thickness of 156 m, which is within the range (100-500 m) postulated by Shackleton (1986). The basaltic layer can be used as a marker horizon to infer buried faults in this area. Trachyte, which is presumed to be the reservoir rock, dominates from 696 m depth and extends to 2384 m, the bottom of the well, with several circulation losses in between the mentioned depths. The formation occurs in seven different varieties based mainly on mineralogical and textural differences as earlier discussed. The trachyte in this well conforms to the plateau trachytes which have been noted to occur in the Olkaria geothermal complex at a depth of 1000 down to 2600 m (Omenda, 2000). No intrusives were encountered in this well.

Well OW-37A shows a systematic occurrence of hydrothermal alteration mineral assemblages. The minerals are mainly present in veins, vesicles and as replacements of primary minerals in the volcanic rocks. The top parts of the well show low-grade alteration represented by chalcedony and zeolites. These assemblages indicate temperatures of less than 180°C. A high-grade assemblage comprising mainly wairakite, prehnite, epidote and actinolite occurs below 616 m, indicating temperatures of >200°C to > 280°C. The mineral deposition sequence is coherent with hydrothermal alteration.

On the basis of hydrothermal alteration minerals and their variation with depth, five hydrothermal mineral zones could be recognized by order of increasing temperature and depth. They are:

(1) The unaltered zone (0-98 m);
(2) Zeolite-chlorite-illite zone (98-626 m);
(3) Chlorite-illite zone (630-1102 m);
(4) Epidote-chlorite-illite (1172-1532 m); and
(5) Actinolite-epidote zone (1550-2384 m).

A study of fluid inclusions in quartz and calcite veins from 668 m depth indicates that the homogenization temperatures lie between 185 and 245°C, and between 170 and 254°C, respectively. A total of 52 inclusions (38 inclusions in quartz and 14 inclusions in calcite) were used in this analysis. A combined fluid inclusion analysis for quartz and calcite established two temperature regimes, 205-220°C and 230-245°C. The formation temperature at this depth (668-670 m) is 248°C. The 205-220°C group of inclusions was formed within the range of alteration temperatures at this depth but was lower than the formation temperature. The 230-245°C inclusions were formed near the existing formation temperature range, hence more recently. Therefore, a comparison of the fluid inclusion homogenization temperatures (T_h) and formation temperature indicates the system has been dynamic as temperature conditions in the system have changed over time. This implies that heating has occurred in the reservoir around well OW-37A at this depth (668-670 m).

Feed zones in this well are interpreted mainly based on circulation losses, high-grade alteration and fracture zones and also on a temperature recovery test which established the well to be open down to the bottom. The heating profile after 17 and 26 days showed a temperature increase at 1100-1200 m and then decreasing temperature down to approximately 2500 m (Figure 23). This was then followed by constant temperature down to the bottom of the well. It appears that water is coming in at 1100-1200 m, and then a trickle below this depth. Several small and medium feed zones occur in the well. These can be deduced from deflections in the temperature profile shown by small to medium peaks indicating the size of the aquifer. Major feed zones occur at 600, 860-1040 and 1100-1480 m. However, it is the aquifer at 1100-1480 m, which is believed to be controlling the well output. The calculated formation temperature in this zone ranges between 266 and 355°C. Pressure profiles further support this fact because the pivot point, which is normally associated with the best feed zone in a well, falls within this zone.

A marker horizon in stratigraphy of wells OW-37A and OW-35 indicates that there is a displacement between these two wells. A normal fault with a total displacement of more than 100 m was observed. Alteration minerals show that alteration zones were found at a shallower depth in well OW-35, caused by a possible shallow cold flow at well OW-37A.

8.2 Conclusions

- The lithology of well OW-37A is composed of pyroclastics, rhyolite, tuffs, basalt and trachytes which conform to the stratigraphic column of the Greater Olkaria volcanic complex as discussed by earlier scholars. No intrusives were encountered in the well.
- The parameters controlling hydrothermal alteration minerals in this field are temperature, permeability and primary rock types.
- Hydrothermal alteration mineralogy indicates temperatures of over 200°C below 616 m, as evidenced by the presence of wairakite, and >280°C below 1548 m, as evidenced by the presence of actinolite. The mineral deposition sequence relates to hydrothermal alteration, showing evolution from low-temperature minerals to high-temperature alteration mineral assemblages with depth.

- Five hydrothermal zonations are recognizable in well OW-37A. They are the unaltered zone, the zeolite-chlorite-illite zone, the chlorite-illite zone, the epidote-chlorite-illite zone, and the actinolite-epidote zone.
- Measurements and studies of fluid inclusions in this well indicate two regimes of alterations, and a comparison of fluid inclusion homogenization temperatures to measured formation temperatures indicates changes in temperature conditions over time. A comparison of the alteration temperature log with the measured formation temperature log indicates the system around well OW-37A has cooled in the upper part down to 600 m and is heating up below that.
- Feed zones in this well are mainly indicated by circulation losses, fracture zones as well as high-grade alteration zones. Small, medium and major feed zones exist in the well. Small and medium aquifers were noticed by small to medium deflections in the temperature profile shown by small to medium peaks. These zones are associated mainly with circulation losses. Major feed zones are indicated by large deflections, hence large peaks in the temperature profile. The main feed zone controlling the well occurs between 1100 and 1480 m. Pressure profiles attest to this fact. Generally, the well has good permeability.

ACKNOWLEDGEMENTS

We offer our sincere appreciation to the UNU, the Government of Iceland, and the KenGen Management. In gratitude, we express our special thanks to Mr. Geoffrey Muchemi (Geothermal Development Manager), Mr. Peketsa Mangi (Chief Officer, Research and Consultancy), and Mr. Fredrick Ongeri (Senior Training Co-ordinator) for granting us the opportunity to participate in the Geothermal Training Programme.

Special appreciation goes to the entire lecturing crew from Iceland GeoSurvey (ISOR); Ms. Anette K. Mortensen, Dr. Björn S. Hardarson, Mr. Sigurdur S, Jónsson, and Mr. Gudmundur H. Gudfinnsson for the enlightenment and impacted knowledge in geothermal science and for painstakingly reading through the manuscript and making very useful suggestions for improvement. It is through them that some of the fundamental problems relating to the project were satisfactorily answered and we particularly cherish their support and advice.

Our very sincere gratitude to our colleagues for their moral support, cooperation and the constructive discussions we held together.

Finally we give all glory and honour to the Almighty Lord for the successful completion of the entire programme.

REFERENCES

Ahmed Y., M., 2008: Borehole geology and hydrothermal mineralization of well HN-08, Hellisheidi geothermal field, SW-Iceland. Report 8 in: *Geothermal training in Iceland 2008*. UNU-GTP, Iceland, 1-29.

Ambusso, W.J., and Ouma, P.A., 1991: Thermodynamic and permeability structure of Olkaria Northeast field: Olkaria fault. *Geothermal Resource Council, Trans.*, 15, 237-242.

Baker, B.H., Mohr, P.A., and Williams, L.A.J., 1972: Geology of the Eastern Rift System of Africa. *Geological Society of America, Special Paper, 136,* 1-67.

Baker, B.H., and Wohlenberg, J., 1971: Structural evolution of the Kenya Rift Valley. *Nature, 229,* 538-542.

Browne, P.R.L., 1978: Hydrothermal alteration in active geothermal fields. *Annual Review Earth and Planetary Science 6,* 229–250.

Browne, P.R.L., 1984a: Subsurface stratigraphy and hydrothermal alteration of Eastern section of the Olkaria geothermal field, Kenya. *Proceedings of the 6th New Zealand Geothermal Workshop, Geothermal Institute, Auckland, NZ*, 33-41.

Browne, P.R.L., 1984b: *Lectures in geothermal geology and petrology*. UNU-GTP, Iceland, report 2, 92 pp.

Clarke, M.C.G., Woodhall, D.G., Allen, D., and Darling G., 1990: *Geological, volcanological and hydrogeological controls on the occurrence of geothermal activity in the area surrounding Lake Naivasha, Kenya, with coloured 1:100 000 geological maps.* Ministry of Energy, Nairobi, 138 pp.

Franzson, H., 2010: *Borehole geology*. UNU-GTP, Iceland, unpublished lecture notes.

Gebrehiwot M., K., 2010: *Subsurface geology, hydrothermal alteration and geothermal model of northern Skardsmýrarfjall, Hellisheidi geothermal field.* University of Iceland, MSc thesis, UNU-GTP, report 5, 65 pp.

Giggenbach, W.F., 1991: Chemical techniques in geothermal exploration. In: D'Amore, F. (coordinator), *Application of geochemistry in geothermal reservoir development*. UNITAR/UNDP publication, Rome, 119-142.

Haukwa, C.B., 1984: *Recent measurements within Olkaria East and West fields*. Kenya Power Co., internal report, 13 pp.

Karingithi, C.W., 1999: *Olkaria Domes geochemical model.* The Kenya Electricity Generating Company, Ltd, internal report, 30 pp.

Karingithi, C.W., 2000: Geochemical characteristics of the Greater Olkaria geothermal field, Kenya. Report 9 in: *Geothermal training in Iceland 2000.* UNU-GTP, Iceland, 165-188.

KenGen 1998: *Surface exploration of Kenya's geothermal resources in the Kenya Rift.* The Kenya Electricity Generating Company, Ltd, internal report, 84 pp.

KenGen 2012: *Geological well logging report for well OW-915B*. KenGen, Kenya, internal report.

Koestono, H., 2007: Borehole geology and hydrothermal alteration of well HE-24, Hellisheidi geothermal field, SW-Iceland. Report 10 in: *Geothermal Training in Iceland, 2007.* UNU-GTP, Iceland, 199-224.

Lagat, J.K., 2004: *Geology, hydrothermal alteration and fluid inclusion studies of the Olkaria Domes geothermal field, Kenya.* University of Iceland, MSc thesis, UNU-GTP, Iceland, report 2, 71 pp.

Lagat, J.K., 2005: Geology, hydrothermal alteration and fluid inclusion studies of Olkaria Domes geothermal field, Kenya. *Proceedings of the World Geothermal Congress 2005, Antalya, Turkey*, 14 pp.

Leach, T.M., and Muchemi G.G., 1987: Geology and hydrothermal alteration of the North and West exploration wells in the Olkaria geothermal field, Kenya. *Proceedings of the 9th New Zealand Geothermal Workshop, Geothermal Institute, Auckland, NZ,* 187-192.

Macdonald, R., Davies, G.R., Bliss, C.M., Leat, P.T., Bailey, D.K. and Smith, R.L., 1987: Geochemistry of high silica peralkaline rhyolites, Naivasha, Kenya rift valley. *J. Petrology, 28,* 979-1008.

Malimo, S.J., 2009: Interpretation of geochemical well test data for wells OW-903B, OW-904B and OW-909, Olkaria Domes field, Kenya. Report 17 in: *Geothermal training in Iceland 2009*. UNU-GTP, Iceland, 319-344.

Mariita, N.O., 2009: Exploration history of Olkaria geothermal field by use of geophysics. *Paper presented at "Short Course IV on Exploration for Geothermal Resources", organized by UNU-GTP, KenGen and GDC, Lake Naivasha, Kenya,* 13 pp.

Mbia, P.K., 2010: Borehole geology and hydrothermal mineralization of well HE-39, Hellisheidi geothermal field, SW-Iceland. Report 19 in: *Geothermal training in Iceland 2010*. UNU-GTP, Iceland, 463-492.

Muchemi, G.G., 1992: *Structural map of Olkaria geothermal field showing inferred ring structures.* Kenya Power Company, internal report.

Muchemi, G.G., 1999: *Conceptual model of the Olkaria geothermal field*. KenGen, internal report, 19 pp.

Muna, Z.W., 1990: *Overview of the geochemistry of the Olkaria West geothermal field, Kenya.* Kenya Power Company, Ltd., internal report, 56 pp.

Mungania, J., 1999: *Geological report of well OW-714*. Kenya Power Company Ltd., internal report.

Mwangi, M.N., 1984: *A review of geophysical data of Olkaria geothermal field for STRM Nov. 1984.* Kenya Power Co., report KPC/4P/OW/007.

Mwangi, M.N., 2000: Country update report for Kenya 1995-1999. *Proceedings of the World Geothermal Conference 2000, Kyoto-Tohoku, Japan,* 327-333.

Naylor, W.I., 1972: *Geology of the Eburru and Olkaria prospects.* UN geothermal exploration project, report.

Ndombi, J.M., 1981: The structure of the shallow crust beneath the Olkaria geothermal field, Kenya, deduced from gravity studies. *J. Volcanol. & Geotherm. Res, 9,* 237-251.

Njue L.M., 2010: Borehole geology and hydrothermal mineralization of well HE-27, Hellisheidi geothermal field, SW-Iceland. Report 24 in: *Geothermal training in Iceland 2010*. UNU-GTP, Iceland, 463-492.

Odongo, M.E.O., 1986: Geology of Olkaria geothermal field. *Geothermics*, *15*, 741-748.

Odongo, M.E.O., 1993: A geological review of Olkaria geothermal reservoir based on structure. *Proceedings of the 15th New Zealand Geothermal Workshop, Geothermal Institute, Auckland,* 169-173 pp.

Ofwona, C.O., 2010: Olkaria 1 reservoir response to 28 years of production. *Proceedings of the World Geothermal Congress 2010*, Bali, Indonesia, 4 pp.

Onacha, S.A., 1993: *Resistivity studies of the Olkaria-Domes geothermal project.* Kenya Power Co., Kenya, internal report.

Omenda, P.A., 1994: The geological structure of the Olkaria west geothermal field, Kenya. *Proceedings of the 19th Stanford Geothermal Reservoir Engineering Workshop, Stanford University, Stanford, Ca,* 125-130.

Omenda, P.A, 1998: The geology and structural controls of the Olkaria geothermal system, Kenya. *Geothermics, 27-1,* 55-74.

Omenda, P.A., 2000: Anatectic origin for Comendite in Olkaria geothermal field, Kenya Rift; Geochemical evidence for syenitic protholith. *African J. Science & Technology, Science and Engineering series, 1,* 39-47.

Shackleton, R.M., 1986: Precambrian collision tectonics in Africa. In: Coward, M.P. and Ries, A.C. (eds.), *Collision Tectonics. Geological Society, Special Publication, 9,* 329-249.

Simiyu, S.M., 1998: Seismic velocity analysis in the Olkaria geothermal field. *Proceedings of the 24th Workshop on Geothermal Reservoir Engineering, Stanford University, Stanford,* 7 pp.

Simiyu, S.M., and Keller, G.R., 1997: An integrated analysis of lithospheric structure across the East African plateau based on gravity anomalies and recent seismic studies. In: Fuchs, K., Altherr, R., Müller, B., and Prodehl, C. (eds.), *Structure and dynamic processes in the lithosphere of the Afro-Arabian rift system*. *Tectonophysics, 278,* 291-313.

Simiyu, S.M., Oduong, E.O., and Mboya, T.K., 1998: *Shear wave attenuation beneath the Olkaria volcanic field.* KenGen, internal report.

Simiyu, S.M., and Malin, P.E., 2000: A "volcanoseismic" approach to geothermal exploration and reservoir monitoring: Olkaria, Kenya and Casa Diablo, USA. *Proceedings of the World Geothermal Congress 2000, Kyushu-Tohoku, Japan,* 1759-1763.

Smith, M., and Mosley, P., 1993: Crustal heterogeneity and basement influence on the development of the Kenya rift, East Africa. *Tectonics, 12,* 591-606.

Thomas, J., 2010: *Fairly simple geology exercises for students and their teachers.* Skidmore College.

Thompson, A.O., and Dodson, R.G., 1963: *Geology of the Naivasha area, Kenya*. Kenya, Geological Survey, report 55.

Thompson, A.J.B., and Thompson, J.F.H (editors), 1996: *Atlas of alteration: A field and petrographic guide to hydrothermal alteration minerals*. Alpine Press Ltd., Vancouver, BC, 119 pp.

Wambugu, J.M., 1995: *Geochemical update of Olkaria West geothermal field.* Kenya Power Company, Ltd., internal report, 40 pp.

Wambugu, J.M., 1996: *Assessment of Olkaria North East geothermal reservoir, based on well discharge chemistry*. Kenya Power Company, internal report.

West-JEC, 2009: *The Olkaria optimization study (phase II)*. West Japan Engineering Consultants, Inc., Optimization development report, 163 pp.

APPENDIX I: XRD ANALYSIS RESULTS

Depth (m)	d(001) OMH	d(001) GLY	d(001) HIT	d(002)	Mineral	Type	Other minerals
56	nd	nd	nd		No clay		
70	nd	nd	nd		No clay		
184	12.24, 10	12.24, 10	12.24, 10	~7 HIT=0	Illite+ unstable chlorite	Unst.chl : ill	
404	nd	nd	nd		No clay		
422	nd	nd	nd		No clay		
444	nd	nd	nd		No clay		
464	nd	nd	nd		No clay		
484	14.18	14.18	14.18	~7 HIT=0	Unstable chlorite	Unst. chl	
542	14.49	14.49	14.49	~7 HIT=0	Unstable chlorite	Unst. chl	
568	14.28, 9.95	14.28, 9.95	14.28, 9.95	~7 HIT=0	Unsta.chlorite, illite	Unst.chl : ill	
606	nd	nd	nd		No clay		
634	14.03	14.03	14.03	~7 HIT=0	Unstable chlorite	Unst chl	
638	14.86	14.86	14.86	~7 HIT=0	Unstable chlorite	Unst chl	
664	14.5	14.5	14.5	~7 HIT = med (7.4)	Chlorite	Chl	
686	14.28, 9.94	14.28, 9.94	14.28, 9.94	~7 HIT=1	Unstable chlorite + Illite	Unst.chl : ill	
708	14.27, 10.06	14.27, 10.06	14.27, 10.06	~7 HIT = low 7.09	Unstable chlorite + Illite	Unst.chl : ill	
728	nd	nd	nd		No clay	Unst. chl	
748	nd	nd	nd		No clay		
762	nd	nd	nd		No clay		
786	12.6	12.6	12.6	~7 HIT=0	Unstable chlorite	Unst. chl	Feldspars
806	12.53	12.53	12.53	~7 HIT=0	Unstable chlorite	Unst. chl	Feldspars
836	12.17	12.17	12.17	~7 HIT=0	Unstable chlorite	Unst. chl	Feldspars
876	nd	nd	nd		No clay	Unst. chl	Feldspars
896	10.02	10.02	10.02		Illite	Illite	
930	14.57	14.57	14.57	~7 HIT=0	Unstable chlorite	Unst. chl	Feldspars
1004	14.45, 10.08	14.45, 10.08	14.45, 10.08	~7 HIT=0	Unstable chlorite + Illite	Unst.chl : ill	Feldspars
1014	14.11, 10.08	14.11, 10.08	14.11, 10.08	~7 HIT=0	Unstable chlorite + Illite	Unst.chl : ill	Feldspars
1028	14.53	14.53	14.53	~7 HIT=0	Unstable chlorite	Unst. chl	Feldspars
1058	14.23	14.23	14.23	~7 HIT=0	Unstable chlorite	Unst. chl	Feldspars
1090	14.08	14.08	14.08	~7 HIT=0	Unstable chlorite	Unst. chl	Feldspars

Depth (m)	d(001) OMH	d(001) GLY	d(001) HIT	d(002)	Mineral	Type	Other minerals
1198	14.04	14.04	14.04	~7 HIT=0	Unstable chlorite	Unst. chl	Feldspars
1200	14.3	14.3	14.3	~7 HIT=0	Unstable chlorite	Unst. chl	Feldspars
1224	14.26, 10.08	14.26, 10.08	14.26, 10.08	~7 HIT=0	Unstable Chlorite, illite	Unst.chl : ill	Feldspars
1478	14.38, 10.08	14.38, 10.08	14.38, 10.08	~7 HIT=0	Unstable Chlorite, illite	Unst.chl : ill	Feldspars
1508	14.23, 104	14.23, 104	14.23, 104	~7 HIT=0	Unstable Chlorite, illite	Unst.chl : ill	Feldspars
1586	14.26, 10.08	14.26, 10.08	14.26, 10.08	~7 HIT = low 7.1	Chlorite + illite	Chl : ill	Amphiboles
1738	14.01, 10.12	14.01, 10.12	14.01, 10.12	~7 HIT=0	Unstable Chlorite, illite	Unst.chl : ill	Amphiboles
1770	15.59, 10.1	15.59, 10.1	15.59, 10.1	~7 HIT = med 7.11	Chlorite + illite	Chl : ill	Amphiboles
1818	12, 10.01	12, 10.01	12, 10.01	~7 HIT=0	Unstable chlorite, illite	Unst.chl : ill	Feldspars
1862	12.18, 10.01	12.18, 10.01	12.18, 10.01	~7 HIT = low 7.1	Chlorite+illite	Chl : ill	
1880	14.53, 10.12	14.53, 10.12	14.53, 10.12	~7 HIT = low 7.15	Chlorite+illite	Chl: ill	
1894	12.15, 10.12	12.15, 10.12	12.15, 10.12	~7 HIT = low 7.08	Chlorite+illite	Chl : ill	
1906	12.05, 10.05	12.05, 10.05	12.05, 10.05	~7 HIT = low 7.08	Chlorite+illite	Chl : ill	Feldspars
1938	12.18, 10.23	12.18, 10.23	12.18, 10.23	~7 HIT = low 7.1	Chlorite+illite	Chl : ill	Feldspars
1982	14.23, 10.12	14.23, 10.12	14.23, 10.12	~7 HIT = med 7.08	Chlorite+illite	Chl : ill	Feldspars
2050	14.15, 9.99	14.15, 9.99	14.15, 9.99	~7 HIT = low 7.1	Chlorite+illite	Chl : ill	Feldspars
2094	14.57, 10.2	14.57, 10.2	14.57, 10.2	~7 HIT = low 7.07	Chlorite+illite	Chl : ill	Feldspars
2208	10.04	10.04	10.04	~7 HIT=l0	Illite and traces unstable chlor.	Illite	
2246	10.12	10.12	10.12		Illite and traces unstable chlor.	Illite	
2268	10.19	10.19	10.19		Illite and traces unstable chlor.	Illite	
2296	10.14	10.14	10.14		Illite and traces unstable chlor.	Illite	
2316	10.27	10.27	10.27		Illite and traces unstable chlor.	Illite	

APPENDIX II: FLUID INCLUSION ANALYSIS RESULTS

Temperature range (°C)	Number of inclusions		
	Quartz 1	Quartz 2	Calcite 1
170-175			1
175-180			
180-185			
185-190		2	
190-195			1
195-200		1	
200-205			3
205-210		6	2
210-215		7	
215-220	1		4
220-225	1	2	
225-230		2	
230-235	4	5	
235-240	3		2
240-245	4		1
245-250			
Sub- total	13	25	14
Total	**52**		

APPENDIX III: STRATIGRAPHY OF WELL OW-37A

Depth (m)	Description	Rock type	Alteration minerals
0-6	Brownish yellow, fine-grained pyroclastics. Composed of mixture of volcanic glass, tuff and pumice fragments. It is slightly oxidized.	Pyroclastics	Clays, oxides
6-18	Greyish, fine-grained, pyroclastics mainly consisting pumice volcanic glass and tuff. It is felsic and slightly oxidized.	Pyroclastics	Clays, oxides
18-22	Yellowish, fine-grained, silicic pyroclastics mainly composed of obsidian (volcanic glass), tuff and glass pumice. It is slightly oxidized.	Pyroclastics	Clays, oxides
22-26	Loss of circulation returns.	-	-
26-32	Yellowish, fine-grained, silicic pyroclastics mainly composed of obsidian (volcanic glass), tuff and glass pumice. It is slightly oxidized.	Pyroclastics	Clays, oxides
32-44	Loss of circulation returns	-	-
44-60	Greyish, fine-grained, felsic, weakly porphyritic rock. It shows lamellar flow and appears slightly oxidized.	Rhyolite	Clays, oxides, pyrite
60-82	Light grey, fine-grained felsic lava. Tinges of iron oxides are noted.	Rhyolite	Clays, pyrite
82-100	Light grey, fine-grained felsic lava. It is moderately porphyritic with phenocrysts of feldspars, iron oxides and quartz. It shows slight oxidation to tinges of iron oxides.	Rhyolite	Clays, analcime, pyrite
100-106	Light grey, fine-grained, felsic lava. It is moderately porphyritic with phenocrysts of feldspars and quartz.	Rhyolite	Clays, analcime, chalcedony
106-298	Loss of circulation returns.	-	-

Depth (m)	Description	Rock type	Alteration minerals
298-304	Light grey, fine-grained, moderately porphyritic rock with phenocrysts of feldspar and quartz. It is felsic and appears slightly oxidized.	Rhyolite	Pyrite, calcite, clay
304-308	Whitish, fine grained, highly porous with pores infilled with calcite, pyrite and clays.	Tuff	Pyrite, clay
308-316	Greyish, fine-grained, highly porphyritic lava. It contains mafic phenocrysts probably of pyroxene. Also, it is veined, fractured and slightly oxidized, in addition to showing lamellae flow.	Trachyte	Pyrite, clay
316-332	Loss of circulation returns	-	-
332-336	Greyish fine-grained highly porphyritic lava. It contains mafic phenocrysts of oxides and pyroxene. Also, it is veined, fractured and slightly oxidized, in addition to showing lamellae flow.	Trachyte	Pyrite, clay
336-342	Loss of circulation returns	-	-
342-356	Light brown, fine-grained felsic lava. It is highly porphyritic with phenocrysts of oxides, feldspars, pyroxenes and quartz. Hematite is noted. It is fractured and slightly altered to clays.	Trachyte	Clays, pyrite, sec. quartz
356-360	Light grey fine-grained, highly porphyritic lava. It is feldspar rich and contains phenocrysts of quartz, pyroxenes and iron oxide. It is moderately fractured and veinlets noted.	Trachyte	Clay, pyrite
360-362	Same, but highly oxidized and fractured.	Trachyte	Pyrite, clay
362-364	Greyish, fine-grained and slightly porphyritic lava with phenocrysts of iron oxide. It is moderately fractured and oxidized along fractures.	Trachyte	Pyrite, clay
364-376	Light grey, fine-grained lava mainly a mixture of minor trachyte and tuff fragments. Green clays are noted.	Tuff	Calcite, pyrite
376-384	Light grey, fine-grained and highly fractured rock. Some grains appear vesicular and the formation also appears laminated. Green clays are noted.	Tuff	Clays
384-392	Same, but highly oxidized with fresh volcanic glass fragments indicative of dikes. Minor calcite and veining is noted.	Tuff	Clays, calcite (minor)
392-396	Light grey, fine-grained and moderately porphyritic rock with phenocrysts of sanidine and pyroxene. Lamination is noted in some grains.	Tuff	Clays, chalcopyrite, pyrite
396-402	Light grey, fine-grained, felsic and slightly porphyritic rock with phenocrysts of iron oxides, pyrite and pyroxene. Slightly oxidized and fractured.	Tuff	Clays, chalcopyrite, pyrite
402-406	Light grey to whitish, fine-grained rock. It is weakly porphyritic with pyrite cubes and pyroxene phenocrysts. Shows pyrite being altered to chalcopyrite.	Tuff	Clays, chalcopyrite, pyrite
406-408	Same, but less altered and less pyrite.	Tuff	Clays, Chalcop., pyrite
408-430	Light grey to whitish, fine-grained rock. It is highly vesicular with no infilling and highly fractured with pyrite and iron oxides infilling the veins. Weakly porphyritic with phenocrysts of quartz and feldspars, probably sanid.	Rhyolitic tuff	Clay (minor), pyrite

Depth (m)	Description	Rock type	Alteration minerals
430-440	Light grey, fine-grained and slightly porphyritic rock with phenocrysts of pyrite, quartz and feldspars. It is slightly fractured.	Rhyolitic tuff	Clay (minor), pyrite, sec. quartz
440-448	Light grey, fine-grained and slightly porphyritic rock with phenocrysts of plagioclase laths. It is slightly fractured and vesicular with pyrite, quartz and iron oxide infillings.	Trachytic tuff	Clay (minor), pyrite, sec. quartz
448-454	Greyish, fine-grained and slightly porphyritic rock with phenocrysts of feldspars. It is vesicular with pyrite and quartz infillings.	Trachytic tuff	Clay (minor), pyrite, sec. quartz
454-456	Same but light grey in colour.	Trachytic tuff	Clay (minor), pyrite, sec.quartz
456-460	Light grey, fine-grained and slightly porphyritic rock. Plagioclase forms the phenocrysts. It is slightly fractured and vesicular with pyrite cubes and quartz infillings.	Trachytic tuff	Clay (minor), pyrite, sec. quartz
460-466	Ditto but moderately porphyritic.	Trachytic tuff	Clay (minor), pyrite, sec.quartz
466-468	Light grey, fine-grained and slightly porphyritic rock. Plagioclase forms the phenocrysts. It is slightly fractured and vesicular with minor pyrite cubes and quartz infillings.	Trachytic tuff	Clay (minor) pyrite, sec. quartz
468-474	Greyish fine-grained moderately porphyritic lava with euhedral plagioclase laths and quartz as phenocrysts. It is vesicular with quartz and pyrite infillings and slightly fractured. It is vesicular with calcite infillings.	Basalt	Clay (minor) pyrite, sec. quartz
474-482	Greyish fine-grained moderately porphyritic lava with phenocrysts of feldspar, quartz, pyrite and calcite. It is highly fractured and vesicular with calcite and clay infillings.	Basalt	Clay (minor), pyrite, sec. quartz calcite
482-504	Dark grey fine-grained moderately porphyritic lava with phenocrysts of feldspar. Calcite infilled vesicles are noted. Needles and crystals of plagioclase are noted.	Basalt	Chlorite, pyrite, sec. quartz, calcite
504-536	Greyish, fine grained, moderately porphyritic with phenocrysts of plagioclase. Calcite infilled vesicles and veins are noted. It is highly fractured.	Basalt	Chlorite, Pyrite Sec. quartz, Calcite
536-540	Greyish fine-grained mixed cuttings mainly basalt and minor light grey vesicular felsic material probably tuff.	Basalt	Chlorite, pyrite, sec. quartz, calcite
540-552	Light grey fine-grained, vesicular and moderately altered to clays. It is fractured and veined with clay infillings.	Tuff	Chlorite, pyrite, se.quartz, calcite
552-572	Greyish-brown fine grained, weakly porphyritic with phenocrysts of plagioclase and pyroxenes. Calcite is abundant in vesicles and fractures and pyrite is disseminated in the rock matrix. Altered olivine noted.	Basalt	Chlorite, illite, pyrite, sec. quartz, calcite
572-582	Dark greyish brown fine-grained weakly porphyritic lava with phenocrysts of feldspars. Vein fillings and vesicles infilled with calcite are noted. Pyrite is disseminated in the whole rock matrix. The formation is moderately fractured and mineral zoning is noted in the vesicles.	Basalt	Chlorite, illite, pyrite, sec. quartz, calcite

Depth (m)	Description	Rock type	Alteration minerals
582-586	Whitish to light grey fine-grained lava. Phenocrysts of pyrite and vesicles noted.	Rhyolitic tuff	Chlorite, illite pyrite, sec. quartz, calcite
586-598	Light grey fine-grained and vesicular lava with clay, calcite and pyrite infillings. It is slightly altered.	Rhyolitic tuff	Chlorite, illite, pyrite, sec. quartz, calcite
598-602	Greyish brown fine-grained vesicular rock with pyrite dissemination in the rock matrix. It is weakly porphyritic with phenocrysts of feldspars. Vesicles and veins infilled with calcite are noted.	Basalt	Chlorite, illite, pyrite, sec. quartz, calcite
602-616	Greyish brown fine-grained vesicular rock with pyrite dissemination in the rock matrix. It is weakly porphyritic with phenocrysts of feldspars. Vesicles and veins infilled with calcite are noted as well as reddish-brown patches of iron oxides.	Basalt	Chlorite, pyrite, sec. quartz, calcite
616-626	Light grey fine-grained rock with phenocrysts of plagioclase. It is highly altered and fractures infilled with pyrite are noted.	Tuff	Chlorite, pyrite, sec. quartz, calcite, wairakite
626-630	Loss of returns	-	-
630-646	Light grey fine-grained rock with plagioclase and clay phenocrysts. It is slightly altered and has fractures infilled with clays, calcite and pyrite.	Tuff	Chlorite, pyrite, sec. quartz, calcite
646-650	Loss of returns.	-	-
650-654	Light grey fine-grained rock with plagioclase and clay phenocrysts. It is slightly altered and has fractures infilled with clays, calcite and pyrite.	Acid tuff	Chlorite, pyrite calcite
654-660	Loss of returns.	-	-
660-668	Dark greyish fine-grained and vesicular lava.	Acid tuff	Chlorite, calcite (abund.)
668-682	Light grey fine-grained moderately porphyritic rock with feldspar phenocrysts. Vesicles infilled with clay and calcite are noted as well as veins infilled with pyrite.	Acid tuff	Chlorite, sec. quartz, pyrite
682-686	Loss of returns.	-	-
686-696	Light grey fine-grained moderately porphyritic rock with feldspar phenocrysts. Vesicles infilled with clay and calcite are noted as well as veins infilled with pyrite.	Acid tuff	Chlorite, illite, sec. quartz, pyrite
696-710	Greyish brown fine-grained slightly porphyritic lava with phenocrysts of feldspars. Pyrite cubes, greenish clays as well as minor secondary quartz are noted.	Trachyte	Chlorite, illite, sec. quartz, Prehnite
710-718	Same but less altered.	Trachyte	Chlorite, sec. quartz, Pyrite
718-732	Light greyish to brown fine-grained slightly porphyritic lava with feldspar and pyroxene phenocrysts. It is slightly fractured and pyrite dissemination in the matrix is noted.	Trachyte	Chlorite, calcite, Pyrite
732-740	Same but less altered.	Trachyte	Calcite, pyrite
740-744	Loss of circulation returns.	-	-
744-746	Light grey fine-grained slightly porphyritic rock with phenocrysts of quartz, feldspar, and pyrite cubes.	Tuff	Sec. quartz, pyrite
746-748	Loss of circulation returns.	-	-

Depth (m)	Description	Rock type	Alteration minerals
748-752	Light grey fine-grained slightly porphyritic rock with phenocrysts of quartz, feldspar, and pyrite cubes. It is weakly altered and veinlets are noted.	Tuff	Sec. quartz, pyrite
752-770	Greyish fine-grained weakly porphyritic lava with phenocrysts of quartz and feldspars. Minor veinlets and fractures are present, including pyrite cubes. The feldspar phenocrysts are fractured along the cleavage planes.	Trachyte	Sec. quartz, pyrite
770-776	Loss of circulation returns.	-	-
776-798	Greyish, fine-grained weakly porphyritic lava with plagioclase, quartz and pyrite cubes phenocrysts. It is fractured and veinlets are also observed.	Trachyte	Chlorite, pyrite
798-814	Same but less oxidized and contain abundant feldspar phenocrysts.	Trachyte	Chlorite, pyrite, siderite
814-818	Loss of circulation returns.	-	-
818-834	Greyish, fine-grained weakly porphyritic lava with plagioclase, quartz and pyrite cubes phenocrysts. It is fractured and veinlets are also observed.	Trachyte	Chlorite, pyrite
834-838	Greyish to brownish fine-grained slightly porphyritic lava with phenocrysts of feldspars, probably sanidine. It is slightly fractured and moderately oxidized.	Trachyte	Chlorite, pyrite
838-852	Same, but slightly oxidized.	Trachyte	Chlorite, pyrite
852-866	Greyish to brownish fine-grained slightly porphyritic lava with phenocrysts of feldspars, probably sanidine. It is slightly fractured and highly oxidized.	Trachyte	Chlorite, pyrite
866-870	Greyish to light brown fine- to medium-grained rock. It is feldspar rich and moderately porphyritic with feldspar and mafic minerals phenocrysts. It is highly fractured, veined and moderately oxidized.	Trachyte	Chlorite, pyrite, sec. quartz
870-890	Brownish fine-grained moderately porphyritic rock with feldspar phenocrysts. It is vesicular with pyrite cubes and green clays infilling vesicles. It is veined, moderately oxidized and highly fractured.	Trachyte	Chlorite, pyrite, sec. quartz
890-894	Light grey fine-grained moderately porphyritic lava with feldspar phenocrysts. It is slightly fractured.	Trachyte	Chlorite, pyrite
894-900	Brownish to greyish fine-grained, weakly porphyritic rock with phenocrysts of feldspars. It is slightly fractured and quartz infilled vesicles are noted. Pyrite cubes are also noted.	Trachyte	Chlorite, illite, pyrite
900-914	Brownish to greyish fine-grained, weakly porphyritic rock with phenocrysts of feldspars. It is fractured and micro-veins are noted.	Trachyte	Chlorite, illite pyrite, sec. quartz
914-930	Greyish fine-grained highly vesicular lava with clay and pyrite infilling the vesicles. It is fractured and veined. Pyrite cubes are also noted.	Trachyte	Chlorite, illite, Pyrite, sec. quartz
930-946	Greyish, fine-grained highly porphyritic lava with feldspar phenocrysts. It is slightly oxidized and the feldspar grains are fractured.	Trachyte	Chlorite, pyrite
946-958	Same, but has pyrite disseminated in the matrix and veins infilled with pyrite.	Trachyte	Chlorite, pyrite

Depth (m)	Description	Rock type	Alteration minerals
958-972	Greyish to brownish, fine-grained and highly porphyritic lava with feldspar phenocrysts. The latter appears fractured, minor pyrite cubes are noted.	Trachyte	Chlorite, pyrite
972-982	Brownish, fine-grained and slightly porphyritic lava with feldspar phenocrysts. It is highly oxidized, slightly fractured and veins infilled with feldspars and clays noted.	Trachyte	Chlorite, pyrite
982-988	Greyish to greenish, fine-grained moderately porphyritic lava with pyrite cubes and feldspar phenocrysts. Also, veins infilled with feldspars are noted.	Trachyte	Chlorite, pyrite
988-994	Same, but more oxidized.	Trachyte	Chlorite, pyrite
994-1004	Greyish, fine-grained slightly porphyritic lava with phenocrysts of feldspars and pyrite. It is slightly fractured.	Trachyte	Chlorite, pyrite
1004-1010	Greyish brown, fine-grained and highly porphyritic lava with phenocrysts of feldspar, pyrite and magnetite. It is moderately oxidized and fractured with veinlets of clay.	Trachyte	Chlorite, illite sec. quartz, pyrite
1010-1014	Same, but with more vein infillings and highly fractured.	Trachyte	Chlorite, sec. quartz, illite, chalcopyrite, pyrite, calcite
1014-1018	Same, but rich in calcite and green clays.	Trachyte	Chlorite, sec. quartz, illite, chalcopyrite, pyrite, calcite
1018-1026	Greyish to brownish, fine-grained, and highly porphyritic lava with phenocrysts of feldspar and pyrite cubes. It is slightly fractured and veins infilled with feldspars and iron oxides (probably siderite) are noted.	Trachyte	Chlorite, pyrite
1026-1028	Same, but has calcite.	Trachyte	Chlorite, pyrite
1028-1034	Greyish to brownish fine-grained highly porphyritic lava with feldspar phenocrysts. It is slightly fractured and moderately oxidized to reddish-brown patches.	Trachyte	Chlorite, pyrite, sec. quartz
1034-1038	Light grey, fine-grained lava. It is fractured with clay and pyrite infilling the fractures. It is highly altered to clays and pyrite is disseminated in the matrix.	Trachyte	Chlorite, pyrite
1038-1042	Brownish grey, fine-grained highly porphyritic lava with phenocrysts of feldspars. It is weakly fractured.	Trachyte	Chlorite, pyrite
1042-1048	Loss of circulation returns.	-	-
1048-1056	Brownish, fine-grained and highly porphyritic lava with phenocrysts of feldspars that appears fractured. Veinlets infilled with pyrite and clays are noted.	Trachyte	Chlorite, pyrite, sec. quartz
1056-1058	Loss of circulation returns.	-	
1058-1062	Brownish, fine-grained moderately porphyritic lava with phenocrysts of feldspars and quartz. It is fractured and veined with pyrite, clay and feldspars infilling the veins.	Trachyte	Chlorite, pyrite, sec. quartz
1062-1070	Greyish, fine-grained slightly porphyritic lava with large feldspar phenocrysts. Minor clays as well as veins infilled with pyrite are noted.	Trachyte	Chlorite, pyrite, sec. quartz Chalcopyrite
1070-1076	Greyish to greenish fine-grained lava. It is slightly fractured and pyrite cubes noted and feldspar phenocrysts.	Trachyte	Chlorite, pyrite, sec. quartz

Depth (m)	Description	Rock type	Alteration minerals
1076-1078	Same, but more oxidized and fractured.	Trachyte	Chlorite, pyrite, sec. quartz
1078-1086	Light grey to greenish fine-grained lava. Pyroxene and feldspar phenocrysts are noted. It is fractured with veinlets of pyrite and clays.	Trachyte	Chlorite, pyrite, sec. quartz
1086-1088	Same, but more oxidized.	Trachyte	Chlorite, pyrite, sec. quartz
1088-1092	Same, but less oxidized.	Trachyte	Chlorite, pyrite, sec. quartz
1092-1098	Loss of circulation returns.	-	-
1098-1102	Light grey to greenish fine-grained lava. Pyroxene and feldspar phenocrysts are noted. It is fractured with veinlets of pyrite and clays.	Trachyte	Chlorite, pyrite, sec. quartz
1102-1172	Loss of circulation returns.	-	-
1172-1180	Greyish to brownish fine to medium-grained highly porphyritic lava with phenocrysts of feldspars. It is slightly fractured.	Trachyte	Chlorite, pyrite, sec. quartz, Epidote
1180-1184	Same, but with calcite.	Trachyte	Chlorite, pyrite, sec. quartz, epidote
1184-1192	Greyish to greenish, fine-grained slightly porphyritic lava with phenocrysts of feldspar and quartz. It is slightly fractured and slightly altered.	Trachyte	Chlorite, pyrite, sec. quartz, epidote, calcite
1192-1210	Same, but more oxidized.	Trachyte	Chlorite, pyrite, sec. quartz, epidote, calcite
1210-1216	Light grey fine-grained slightly porphyritic lava. Contains feldspar and pyrite cubes phenocrysts. Slightly fractured and veinlets infilled with pyrite noted. Slightly altered.	Trachyte	Chlorite, pyrite sec. quartz, epidote
1216-1220	Same, but more oxidized and abundant pyrite cubes.	Trachyte	Chlorite, pyrite, Sec. quartz, epidote
1220-1240	Same, but highly oxidized.	Trachyte	Chlorite, illite, pyrite, sec. quartz, epidote
1240-1246	Light greenish to grey, fine-grained slightly porphyritic lava with phenocrysts of feldspars and pyrite cubes. It is veined and contains vesicles infilled with calcite.	Trachyte	Chlorite, illite, pyrite, sec. quartz, calcite
1246-1360	Loss of circulation returns.	-	-
1360-1364	Greyish fine-grained slightly porphyritic lava with vesicles infilled with quartz. It is veined, slightly oxidized and pyrite is disseminated in the rock matrix.	Trachyte	Chlorite, illite, pyrite, sec. quartz
1364-1368	Loss of circulation returns.	-	-
1368-1370	Greenish to greyish fine-grained slightly porphyritic lava with phenocrysts of feldspars. Abundant epidote is noted.	Trachyte	Chlorite, illite, epidote, sec. quartz
1370-1502	Loss of circulation returns.	-	-
1502-1532	Grey to brown, fine-grained, moderately porphyritic rock with phenocrysts of feldspar. The formation is slightly oxidized and slightly fractured with minor vein fillings.	Trachyte	Chlorite, illite, hematite pyrite

Depth (m)	Description	Rock type	Alteration minerals
1532-1548	Loss of circulation returns.	-	-
1548-1554	Light grey, fine-grained, highly porphyritic lava with phenocrysts of sanidine. The formation is nearly fresh with few feldspar phenocrysts being lightly altered to clays. Veinlets infilled with clay and feldspar noted.	Trachyte	Chlorite, illite, epidote, sec. quartz, actinolite
1554-1560	Loss of circulation returns.	-	-
1560-1562	Light grey, fine-grained, highly porphyritic lava with phenocrysts of sanidine. The formation is nearly fresh with few feldspar phenocrysts being lightly altered to clays. Veinlets infilled with clay and feldspar noted.	Trachyte	Chlorite, illite, epidote, sec. quartz, actinolite
1562-1578	Loss of circulation returns.	-	-
1578-1582	Light grey, fine-grained, highly porphyritic lava with phenocrysts of sanidine. The formation is nearly fresh with few feldspar phenocrysts being lightly altered to clays. Veinlets infilled with clay and feldspar noted.	Trachyte	Chlorite, illite, epidote, sec. quartz, calcite actinolite
1582-1592	Loss of circulation returns.	-	-
1592-1598	Light grey, fine-grained, highly porphyritic lava with phenocrysts of sanidine. The formation is nearly fresh with few feldspar phenocrysts being lightly altered to clays. Veinlets infilled with clay and feldspar noted.	Trachyte	Chlorite, illite, Epidote, sec. quartz, calcite, actinolite
1598-1614	Loss of circulation returns.	-	-
1614-1626	Light grey, fine-grained, highly porphyritic lava with phenocrysts and laths of sanidine. The formation is nearly fresh with few feldspar phenocrysts being lightly altered to clays. Veinlets infilled with clay and feldspar noted.	Trachyte	Chlorite, illite Pyrite, hematite actinolite
1626-1632	Grey, fine-grained, slightly porphyritic lava with phenocrysts and laths of sanidine. Veinlets infilled with pyrite and hematite are noted.	Trachyte	Chlorite, illite, pyrite, hematite, actinolite
1632-1654	Loss of circulation returns.	-	-
1654-1660	Grey to brown, fine-grained lava with porphyries of feldspars. It is moderately oxidized and fractured with veins that have been filled with clays. Pyrite cubes noted.	Trachyte	Chlorite, illite, pyrite, actinolite
1660-1668	Loss of circulation returns.	-	-
1668-1676	Light grey with some brown oxidation clays and slightly oxidized. Formation slightly fractured with few veinlets.	Trachyte	Chlorite, illite, pyrite, actinolite
1676-1678	Same, but less oxidized.	Trachyte	Chlorite, illite, pyrite, actinolite
1678-1730	Loss of circulation returns.	-	-
1730-1740	Greyish, fine-grained, slightly porphyritic lava. The formation is slightly altered to brown and green clays. Minor pyrite cubes and spherulites are noted. Few veinlets are noted.	Trachyte	Chlorite, illite, actinolite
1740-1762	Loss of circulation returns.	-	-
1762-1766	Grey, fine-grained, slightly porphyritic lava with laths and phenocrysts of feldspars. Slightly altered to clay and pyrite is noted in groundmass.	Trachyte	Chlorite, illite, pyrite, sphene, actinolite
1766-1770	Loss of circulation returns.	-	-
1770-1780	Grey, with some brown and green clays, fine-grained lava. Slightly porphyritic lava with phenocrysts of sanidine.	Trachyte	Chlorite, illite, pyrite, sphene, actinolite

Depth (m)	Description	Rock type	Alteration minerals
1780-1788	Same, but less altered.	Trachyte	Chlorite, illite, pyrite, sphene, actinolite
1788-1800	Loss of circulation returns.	-	-
1800-1814	Light grey, feldspar rich, fine-grained lava exhibiting trachytic texture. Formation is nearly fresh with little alteration to clays. Slightly fractured formation with clay vein fillings.	Trachyte	Chlorite, illite, pyrite, sphene, actinolite
1814-1818	Same, but more fractured with more clay vein fillings	Trachyte	Chlorite, illite, actinolite
1818-1824	Dark grey, fine-grained and weakly porphyritic lava with phenocrysts of sanidine. Slightly altered to clays.	Trachyte	Chlorite, illite, actinolite
1824-1834	Light grey to green, feldspar rich, medium- to fine-grained lava. Slightly porphyritic with sanidine phenocrysts. The formation is moderately altered to chlorite and illite clays. Slightly fractured formation with clay vein fillings.	Trachyte	Chlorite, illite sec. quartz, actinolite
1834-1848	Grey, fine-grained, slightly porphyritic lava with phenocrysts of feldspars. Slightly altered to clay and moderately oxidized.	Trachyte	Chlorite, illite sec. quartz, pyrite, actinolite
1848-1860	Loss of circulation returns.	-	-
1860-1866	Grey, cryptocrystalline lava. Appears moderately oxidized and slightly altered to chlorite and illite clays. Slightly fractured with chlorite vein fillings.	Trachyte	Chlorite, illite, pyrite, actinolite
1866-1876	Loss of circulation returns.	-	-
1876-1882	Grey, fine-grained to cryptocrystalline lava. The formation is slightly fractured with veinlets infilled with clay. Slightly vesicular rock with clay infilling.	Trachyte	Chlorite, illite, pyrite, actinolite
1882-1890	Loss of circulation returns.	-	-
1890-1894	Grey, fine-grained to cryptocrystalline lava. The formation is slightly fractured with pyrite, illite and chlorite vein fillings. Slightly vesicular rock with chlorite in-fillings.	Trachyte	Chlorite, illite, pyrite, actinolite
1894-1906	Loss of circulation returns.	-	-
1906-1914	Greyish, medium-grained and highly porphyritic lava with phenocrysts of sanidine. Slightly oxidized and slightly altered to green and brown clays.	Trachyte	Chlorite, illite, pyrite, sphene sec. quartz actinolite
1914-1938	Loss of circulation returns.	-	-
1938-1952	Grey, medium-grained highly porphyritic lava with phenocrysts of sanidine. Slightly fractured with clay vein fillings.	Trachyte	Chlorite, illite, pyrite, sphene, actinolite
1952-1958	Grey, fine-grained, highly porphyritic lava with phenocrysts of sanidine. Slightly fractured with clay vein fillings.	Trachyte	Chlorite, illite, pyrite, sphene, actinolite
1958-1962	Loss of circulation returns.	-	-
1962-1968	Light grey to grey, fine-grained rock. It is porphyritic with subhedral phenocrysts of sanidine. It is slightly oxidized and altered to chlorite and illite clays. Pyrite is disseminated in the groundmass.	Trachyte	Chlorite, illite, pyrite, sphene, actinolite

Depth (m)	Description	Rock type	Alteration minerals
1968-1972	Light grey to grey, fine-grained rock. It is porphyritic with subhedral phenocrysts of sanidine. It is slightly oxidized and altered to chlorite and illite clays. Pyrite is disseminated in the groundmass and veinlets infilled with mafic minerals.	Trachyte	Chlorite, illite, pyrite, sphene, actinolite
1972-1980	Grey to brown, fine-grained, feldspar rich lava. It is moderately oxidized and fractured with clay vein fillings. Vesicles infilled with pale green clays are present.	Trachyte	Chlorite, illite, pyrite, sphene, actinolite
1980-1998	Light grey, feldspar rich, fine-grained to cryptocrystalline rock. Formation moderately altered to chlorite and illite clays. Slightly fractured formation with clay vein fillings.	Trachyte	Chlorite, illite, sphene, actinolite
1998-2006	Light grey, fine-grained, feldspar rich lava. The formation is slightly oxidized and altered to chlorite and illite clays. Slightly fractured formation with clay vein fillings.	Trachyte	Chlorite, illite, pyrite, sec. quartz, hematite, actinolite
2006-2036	Same, but more altered and oxidized.	Trachyte	Chlorite, illite, pyrite, sec. quartz, actinolite
2036-2042	Same, but with pyrite vein fillings.	Trachyte	Chlorite, illite, pyrite, sec. quartz, actinolite
2042-2050	Light grey, feldspar rich, fine-grained to cryptocrystalline rock. The formation is slightly altered to chlorite and illite clays. Slightly fractured formation with clay vein fillings.	Trachyte	Chlorite, illite, pyrite, sec. quartz, actinolite
2050-2056	Same, but more oxidized. Pyrite is also noted.	Trachyte	Chlorite, illite, pyrite, sec. quartz, actinolite
2056-2062	Loss of circulation returns.	-	-
2062-2066	Light grey, feldspar rich, fine-grained to cryptocrystalline rock. The formation slightly altered to chlorite and illite clays. Slightly fractured formation with clay vein fillings.	Trachyte	Chlorite, illite, pyrite, sec. quartz, actinolite
2066-2164	Loss of circulation returns.	-	-
2164-2168	Light grey, fine-grained, feldspar rich lava. The formation is slightly oxidized and nearly fresh formation with traces of chlorite and illite clay alteration. Slightly fractured formation with clay vein fillings.	Trachyte	Chlorite, illite, pyrite, epidote, actinolite
2168-2186	Loss of circulation returns.	-	-
2186-2194	Light grey, fine-grained, feldspar rich lava. The formation is slightly oxidized and moderately altered chlorite and illite clay. Slightly fractured formation with clay vein fillings.	Trachyte	Chlorite, illite, pyrite, epidote, actinolite
2194-2202	Same, but porphyritic with euhedral phenocrysts of sanidine.	Trachyte	Chlorite, illite, pyrite, epidote, actinolite
2202-2204	Loss of circulation returns.	-	-
2204-2212	Light grey, fine-grained, feldspar rich lava. The formation is slightly porphyritic lava with phenocrysts of sanidine. Slightly fractured with clay vein fillings.	Trachyte	Chlorite, illite, pyrite, sec. quartz, hematite, actinolite

Depth (m)	Description	Rock type	Alteration minerals
2212-2216	Loss of circulation returns.	-	-
2216-2224	Light grey, fine-grained, feldspar rich lava. The formation is slightly porphyritic lava with phenocrysts of sanidine. Slightly fractured with clay vein fillings.	Trachyte	Chlorite, illite, pyrite, sec. quartz, hematite, actinolite
2224-2246	Loss of circulation returns.	-	-
2246-2252	Light grey, fine-grained, feldspar rich lava. The formation is slightly porphyritic lava with phenocrysts of sanidine. Slightly fractured with pyrite and illite vein fillings.	Trachyte	Chlorite, illite, pyrite, hematite, actinolite
2252-2268	Loss of circulation returns.	-	-
2268-2280	Light grey, fine-grained, feldspar rich lava. The formation is nearly fresh with traces of illite clay alteration.	Trachyte	Chlorite, illite actinolite
2280-2286	Loss of circulation returns.	-	-
2286-2288	Light grey, fine-grained, feldspar rich lava. The formation is nearly fresh with traces of illite clay alteration.	Trachyte	Chlorite, illite actinolite
2288-2296	Loss of circulation returns.	-	-
2296-2300	Grey, fine- to medium-grained lava. Slightly porphyritic with plagioclase and sanidine phenocrysts.	Trachyte	Chlorite, illite, epidote, actinolite
2300-2304	Loss of circulation returns.	-	-
2304-2308	Grey, fine- to medium-grained lava. Slightly porphyritic with plagioclase and sanidine phenocrysts.	Trachyte	Chlorite, illite, epidote, actinolite
2308-2314	Loss of circulation returns.	-	-
2314-2320	Light grey, fine- to medium-grained feldspar rich lava. Euhedral phenocrysts of sanidine are noted. The formation is moderately altered to illite clay. Slightly fractured with clay vein fillings.	Trachyte	Chlorite, illite, epidote, actinolite
2320-2328	Loss of circulation returns.	-	-
2328-2330	Light grey, fine- to medium-grained feldspar rich lava. Euhedral phenocrysts of sanidine are noted. The formation is moderately altered to illite clay. Slightly fractured with clay vein fillings.	Trachyte	Chlorite, illite, epidote, actinolite
2330-2340	Loss of circulation returns.	-	-
2340-2342	Light grey, fine- to medium-grained feldspar rich lava. Euhedral phenocrysts of sanidine are noted. The formation is moderately altered to illite clay. Slightly fractured with clay vein fillings.	Trachyte	Chlorite, illite, epidote, actinolite
2382-2384	Grey, fine- to medium-grained lava. Slightly porphyritic with sanidine phenocrysts. The rock is slightly fractured with illite and epidote infilling veins.	Trachyte	Chlorite, illite, epidote, actinolite
2384-2848	Loss of circulation returns.	-	-